Mechanism of the ECM stiffness-dependent differentiation of mesenchymal stem cells

Mito KURODA

2018

ABBREBIATIONS

ALP	alkaline phosphatase
aP2	adipocyte protein 2
ArgBP2	Arg-binding protein 2
CAP	c-Cbl-associated protein
ECM	extracellular matrix
ERK	extracellular signal-regulated kinase
FA	focal adhesion
FAK	focal adhesion kinase
F-actin	filamentous actin
G-actin	globular actin
IBMX	3-isobutyl-1-methylxanthine
IRES	internal ribosomal entry site
KD	knockdown
KO	knockout
MEF	mouse embryonic fibroblast
MSC	mesenchymal stem cell
PPARγ	peroxisome proliferator-activated receptor gamma
Runx2	Runt related transcription factor 2
S.E.M.	standard error of the mean
SH3	Src homology 3
shRNA	short hairpin RNA
siRNA	small interfering RNA
SoHo	sorbin homology
TAZ	transcriptional coactivator with a PDZ-binding motif
Vh	vinculin head
Vt	vinculin tail
WT	wild type
YAP	Yes-associated protein

CONTENTS

INTRODUCTION

All multicellular organisms grow and maintain functional tissues with resident stem cells. Mesenchymal stem cells (MSCs) are multipotent stem cells with the capability to differentiate into various types of cells, including neuroblasts, adipocytes, myoblasts, chondrocytes, and osteoblasts (1, 2). For instance, MSCs can be differentiated into adipocytes by stimulation with bone morphogenetic protein (BMP) 4 (3), while into osteoblasts or chondrocytes by treatment with BMP2, a member of TGF-β superfamily protein, and Wnt ligands (4, 5). In addition to soluble factors, MSC lineage specifications can be directed by physical changes induced by the extracellular environment, including cell area and strain, and by stiffness of extracellular matrix (ECM) (6-10). MSCs cultured on soft substrates differentiate into adipocytes efficiently, whereas cells on rigid substrates preferentially differentiate into osteoblasts (6, 7). However, mechanisms underlying the ECM stiffness-dependent differentiation was largely unclear.

Cell-ECM adhesion sites, called focal adhesions (FAs), mechanically link ECM to the actin cytoskeleton and play critical roles in mechanosensing and mechanotransduction. FAs contain ECM receptor proteins, integrins, and cytosolic adaptor proteins, including talin and vinculin. Force-induced conformational changes of FA proteins are thought to key steps to transduce forces to biochemical signals (11). For example, substrate domains of p130CAS (Crk-associated substrate) are extended in response to cell stretching, leading to phosphorylation of CAS by Src family kinases (12). In addition, talin rod domains next to the N-terminal head domain are unfolded by force, enabling talin association with vinculin through vinculin binding sites (VBS) (13).

Vinculin is another major sensor for ECM stiffness (14). Vinculin consists of an N-

terminal head domain (Vh), C-terminal tail domain (Vt), and a linker region connecting these two domains. Vh binds to talin and integrin, while Vt binds to F-actin (15, 16). The linker region binds to Arp2/3, vinexin (also known as SORBS3), CAP (c-Cbl-associated protein, also known as SORBS1) and p130CAS (also known as BCAR1) (17-19). Head-tail intramolecular interaction results in low affinity to F-actin (i.e., closed form of vinculin), while disruption of the interaction leads to conformational changes of vinculin that has higher affinity to F-actin (i.e., open form of vinculin) (20, 21).

It has been previously revealed that vinculin adopts actin-high affinity form on rigid ECM and actin-low affinity form on soft ECM. This regulation requires the binding of vinculin to vinexin α and CAP, two of three SORBS proteins (22). Furthermore, this interaction is necessary for ECM stiffness-dependent cell migration of fibroblasts (23). In addition, p130CAS also affects vinculin retention at FAs through direct interaction (18). Although vinculin, as well as vinexin α and CAP, seem to function as mechanosensors in mouse embryonic fibroblasts, whether vinculin and SORBS proteins regulate the ECM stiffness-dependent differentiation of MSCs to adipocytes is still incompletely understood.

Adipocyte differentiation involves two main steps: lineage commitment and terminal differentiation. MSCs switch into preadipocytes in response to several stimuli as described above. In this step, transcriptional co-activator YAP/TAZ play essential roles in modulating the balance of differentiation in MSCs (24, 25). In the latter step, transcriptional factor peroxisome proliferator-activated receptor-γ (PPARγ) functions as a master regulator for adipogenesis, which drives the expression of several target genes including adipocyte protein-2 (aP2, also known as fatty acid binding protein 4) and glucose transporter type 4 (GLUT4) (26). This activation of PPARγ is required for maturation of adipocytes to serve as lipid storage. Functional adipocytes are essential for maintaining energy and metabolic homeostasis (27). Therefore, it is important to

unveil mechanisms of MSC differentiation into adipocytes in order to understand and improve metabolic syndromes. However, no study has revealed the mechanism of ECM stiffness-dependent differentiation into adipocytes.

The goal of this study is to reveal whether vinculin and SORBS family proteins regulate the ECM stiffness-dependent differentiation into adipocytes and to reveal the mechanism underlying differentiation. In Chapter 1, the author examined the roles of vinculin in the ECM stiffness-dependent differentiation of MSCs into adipocytes and revealed that vinculin inhibits the differentiation via promoting the nuclear localization of YAP/TAZ. In Chapter 2, the author examined the roles of SORBS proteins, vinculin-binding partners, and elucidated that SORBS family proteins play crucial roles in regulating ECM stiffness-dependent differentiation. In addition, the author identified the novel role of vinexin as a regulator of adipogenesis.

REFERENCES

1. Kopen GC, Prockop DJ, & Phinney DG (1999) Marrow stromal cells migrate throughout forebrain and cerebellum, and they differentiate into astrocytes after injection into neonatal mouse brains. *Proc Natl Acad Sci U S A* 96(19):10711-10716.
2. Pittenger MF, *et al.* (1999) Multilineage potential of adult human mesenchymal stem cells. *Science* 284(5411):143-147.
3. Tang QQ, Otto TC, & Lane MD (2004) Commitment of C3H10T1/2 pluripotent stem cells to the adipocyte lineage. *Proc Natl Acad Sci U S A* 101(26):9607-9611.
4. Noël D, *et al.* (2004) Short-term BMP-2 expression is sufficient for in vivo osteochondral differentiation of mesenchymal stem cells. *Stem Cells* 22(1):74-85.
5. Ross SE, *et al.* (2000) Inhibition of adipogenesis by Wnt signaling. *Science* 289(5481):950-953.
6. Dupont S, *et al.* (2011) Role of YAP/TAZ in mechanotransduction. *Nature* 474(7350):179-183.
7. Engler AJ, Sen S, Sweeney HL, & Discher DE (2006) Matrix elasticity directs stem cell lineage specification. *Cell* 126(4):677-689.
8. McBeath R, Pirone DM, Nelson CM, Bhadriraju K, & Chen CS (2004) Cell shape, cytoskeletal tension, and RhoA regulate stem cell lineage commitment. *Dev Cell*

6(4):483-495.

9. Sen B, *et al.* (2009) Mechanical loading regulates NFATc1 and beta-catenin signaling through a GSK3beta control node. *J Biol Chem* 284(50):34607-34617.
10. Swift J, *et al.* (2013) Nuclear lamin-A scales with tissue stiffness and enhances matrix-directed differentiation. *Science* 341(6149):1240104.
11. Roca-Cusachs P, Iskratsch T, & Sheetz MP (2012) Finding the weakest link: exploring integrin-mediated mechanical molecular pathways. *J Cell Sci* 125(Pt 13):3025-3038.
12. Sawada Y, *et al.* (2006) Force sensing by mechanical extension of the Src family kinase substrate p130Cas. *Cell* 127(5):1015-1026.
13. del Rio A, *et al.* (2009) Stretching single talin rod molecules activates vinculin binding. *Science* 323(5914):638-641.
14. Atherton P, Stutchbury B, Jethwa D, & Ballestrem C (2016) Mechanosensitive components of integrin adhesions: Role of vinculin. *Exp Cell Res* 343(1):21-27.
15. Jockusch BM & Isenberg G (1981) Interaction of alpha-actinin and vinculin with actin: opposite effects on filament network formation. *Proc Natl Acad Sci U S A* 78(5):3005-3009.
16. Menkel AR, *et al.* (1994) Characterization of an F-actin-binding domain in the cytoskeletal protein vinculin. *J Cell Biol* 126(5):1231-1240.
17. DeMali KA, Barlow CA, & Burridge K (2002) Recruitment of the Arp2/3 complex to vinculin: coupling membrane protrusion to matrix adhesion. *J Cell Biol* 159(5):881-891.
18. Janoštiak R, *et al.* (2014) CAS directly interacts with vinculin to control mechanosensing and focal adhesion dynamics. *Cell Mol Life Sci* 71(4):727-744.
19. Kioka N, *et al.* (1999) Vinexin: a novel vinculin-binding protein with multiple SH3 domains enhances actin cytoskeletal organization. *J Cell Biol* 144(1):59-69.
20. Johnson RP & Craig SW (1995) F-actin binding site masked by the intramolecular association of vinculin head and tail domains. *Nature* 373(6511):261-264.
21. Cohen DM, Chen H, Johnson RP, Choudhury B, & Craig SW (2005) Two distinct head-tail interfaces cooperate to suppress activation of vinculin by talin. *J Biol Chem* 280(17):17109-17117.
22. Ichikawa T, *et al.* (2017) Vinexin family (SORBS) proteins play different roles in stiffness-sensing and contractile force generation. *J Cell Sci* 130(20):3517-3531.
23. Yamashita H, *et al.* (2014) The role of the interaction of the vinculin proline-rich linker region with vinexin α in sensing the stiffness of the extracellular matrix. *J Cell Sci* 127(Pt 9):1875-1886.
24. Seo E, *et al.* (2013) SOX2 regulates YAP1 to maintain stemness and determine cell fate

in the osteo-adipo lineage. *Cell Rep* 3(6):2075-2087.

25. Hong JH, *et al.* (2005) TAZ, a transcriptional modulator of mesenchymal stem cell differentiation. *Science* 309(5737):1074-1078.
26. Ahmadian M, *et al.* (2013) PPARγ signaling and metabolism: the good, the bad and the future. *Nat Med* 19(5):557-566.
27. Cristancho AG & Lazar MA (2011) Forming functional fat: a growing understanding of adipocyte differentiation. *Nat Rev Mol Cell Biol* 12(11):722-734.

CHAPTER 1

Roles of vinculin in the ECM stiffness-dependent differentiation into adipocytes

CHAPTER 1

Roles of vinculin in the ECM stiffness-dependent differentiation into adipocytes

Vinculin adopts the open form on rigid ECM and the closed form on soft ECM. Although vinculin seems to function as mechanosensors in mouse embryonic fibroblasts, whether vinculin regulates the stiffness-dependent differentiation of MSCs to adipocytes is not understood.

Yes-associated protein (YAP, also known as YAP1) and its paralog transcriptional coactivator with a PDZ-binding motif (TAZ, also known as WWTR1) (hereafter YAP/TAZ) are core components of the mammalian Hippo pathway. YAP/TAZ play a crucial role in regulating cell proliferation and differentiation through transcriptional activation (1). Moderate expression of YAP induces adipogenesis through cooperating with Wnt/β-catenin signaling (2). TAZ modulates the balance of differentiation between adipocytes and osteoblasts in MSCs (3). In addition, physical cues, including cell morphology and ECM stiffness, controls YAP/TAZ subcellular localization and function (4-7). YAP/TAZ is preferentially accumulated within the nucleus and becomes transcriptionally active on rigid ECM to promote osteogenesis, whereas it accumulates within the cytosol on soft ECM (8). Although intracellular tension and actin organization are suggested to be involved in this regulation, the mechanism by which ECM stiffness regulates YAP/TAZ remains poorly clarified.

In this study, the author shows that vinculin functions as a mechanosensor in MSCs and promotes the nuclear localization of the transcription factor TAZ to inhibit the adipocyte differentiation on rigid ECM.

RESULTS

Differentiation of MSCs is regulated by ECM stiffness

The author first examined the effect of ECM stiffness on the adipocyte differentiation of ST2 cells, a mouse bone-marrow-derived stromal cell line. Cells were seeded on collagen-coated polyacrylamide (PAA) gel substrates with different levels of stiffness (1.5 or 8.7 kPa, which corresponds to the stiffness of adipose tissues (9)), and induced to differentiate into adipocytes. Cells on soft substrates (1.5 kPa) expressed higher levels of adipogenic markers, including PPARγ2 (1.5-fold ± 0.16) and aP2 (1.5-fold ± 0.14) (mean ± s.e.m.), than those on rigid substrates (8.7 kPa) (Fig. 1A). Furthermore, soft substrates increased the expression of aP2 protein (Fig. 1B). These data indicate that ECM stiffness regulates the differentiation of ST2 cells into adipocytes, and rigid ECM suppresses adipocyte differentiation.

ST2 cells showed an osteogenic phenotype, as indicated by increased mRNA expression of osteogenic markers, after culturing on rigid (plastic) substrates without adipogenic induction (data not shown). To examine whether ECM stiffness affects the differentiation of ST2 cells into other cell types, expression of markers for osteoblast, chondrocyte and myoblast was also analyzed under this condition. As shown in Fig. 1C, rigid substrates (23 kPa) increased the expression of osteogenic markers, e.g. runt-related transcription factor 2 (Runx2), alkaline phosphatase (ALP, also known as Alpl), and osteopontin (Fig. 1C). The substrates with 8.7 kPa stiffness gave similar results. Likewise, expression of Sox9, a chondrogenic marker, was higher on rigid substrates (Fig. 1D). Expression of MyoD (also known as MyoD1), a myogenic marker, was not affected by the ECM stiffness (Fig. 1E), despite previous reports showing that primary MSCs expressed the highest levels of MyoD on 11 kPa substrates (10). Taken together, these results suggest that ECM stiffness can regulate the commitment of ST2 cells to adipocytes or osteoblasts.

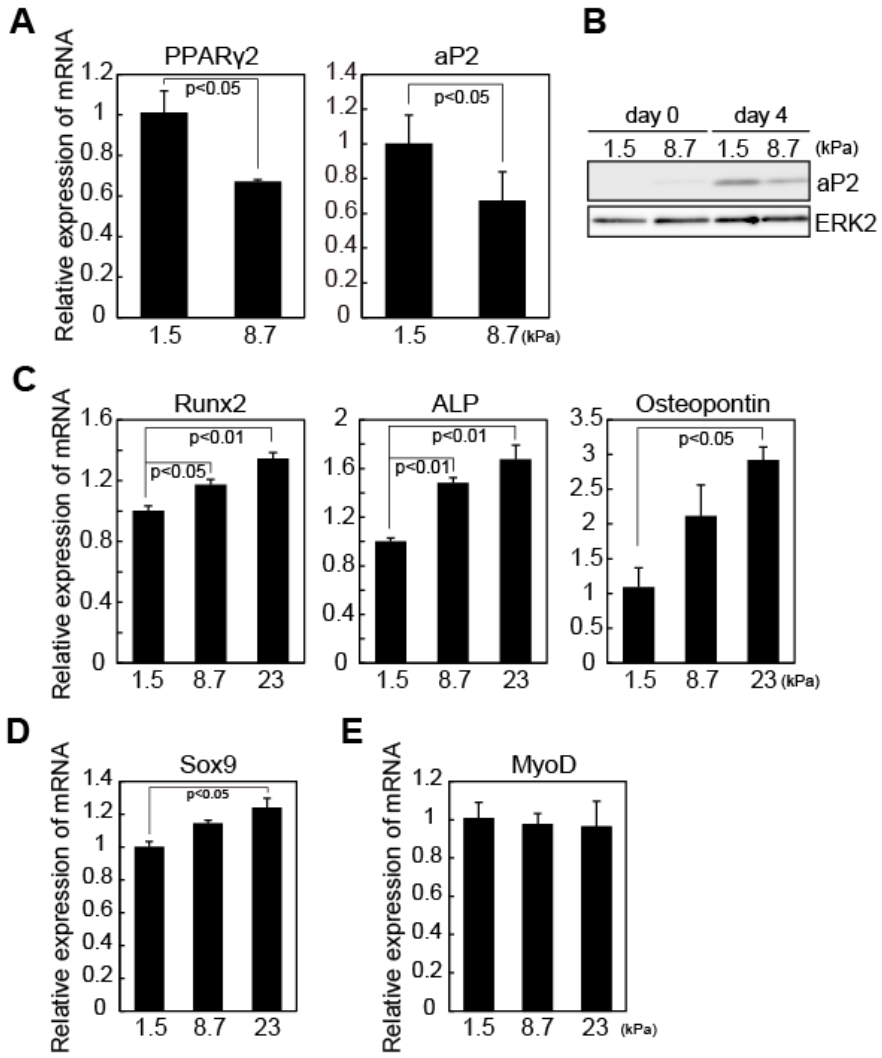

Fig. 1. Rigid ECM suppressed the differentiation of ST2 cells into adipocytes. (A,B) WT ST2 cells were seeded on type I collagen-coated substrates with different levels of stiffness (1.5 kPa, 8.7 kPa) at a density of 7.5×10^4 cells/35 mm dish. After 24 h, cells were differentiated into adipocytes by the addition of the MDI mixture (0.5 mM IBMX, 10 μM DEX and 10 μg/ml insulin). (A) On day 6 after MDI treatment, the expression of mRNA encoding of PPARγ2 and aP2 was quantified by qRT-PCR and normalized to GAPDH expression in triplicate experiments. Relative expression to that on soft substrates is shown in the graphs. (B) On day 4 after MDI treatment, cells were lysed. The amounts of lysates were normalized to the DNA content, and expression of aP2 analyzed by western blotting. ERK2 was used as a loading control. Results are representative of three experiments. (C,D,E) Cells were seeded on type I collagen-coated substrates with different levels of stiffness (1.5 kPa, 8.7 kPa, 23 kPa). At 7 days after seeding, the levels of mRNA expression for indicated genes were quantified by qRT-PCR from triplicate experiments. mRNA expression was normalized to 36B4, and the relative expression to soft substrates is shown. The values represent the mean ± s.e.m. from triplicate experiments. Experiments were performed two (A) or three (C) times. Statistical significance was determined by Student's t-test (A) or one-way ANOVA with Tukey's test (C,D,E).

The resistance of vinculin to CSK treatment changes in a manner dependent on ECM stiffness

Cytoskeleton stabilization buffer (CSK) treatment removes cytoplasmic proteins as well as proteins that are loosely attached to the cytoskeleton from cells, but does not remove proteins that bind tightly to the cytoskeleton. Thus, the amount of cytoskeleton-associated vinculin (open form of vinculin) can be visualized by CSK treatment. Yamashita et al. recently demonstrated that the amount of CSK-resistant vinculin is increased in cells cultured on rigid substrates and that conformational change of vinculin is involved in sensing ECM stiffness in mouse embryonic fibroblasts (11). Thus, the author next examined the effects of ECM stiffness on the resistance of vinculin to CSK treatment in ST2 cells. First, the author determined the localization of vinculin on PAA substrates with different levels of stiffness (1.5 kPa, 3.2 kPa, and 8.7 kPa) by normal immunostaining, that is, without CSK treatment (Fig. 2A). Quantified data show that the number and the area of vinculin-containing FAs per cell were comparable on all of the levels of stiffness tested (Fig. 2B). The integrated intensity of vinculin at FA was also comparable for each level of

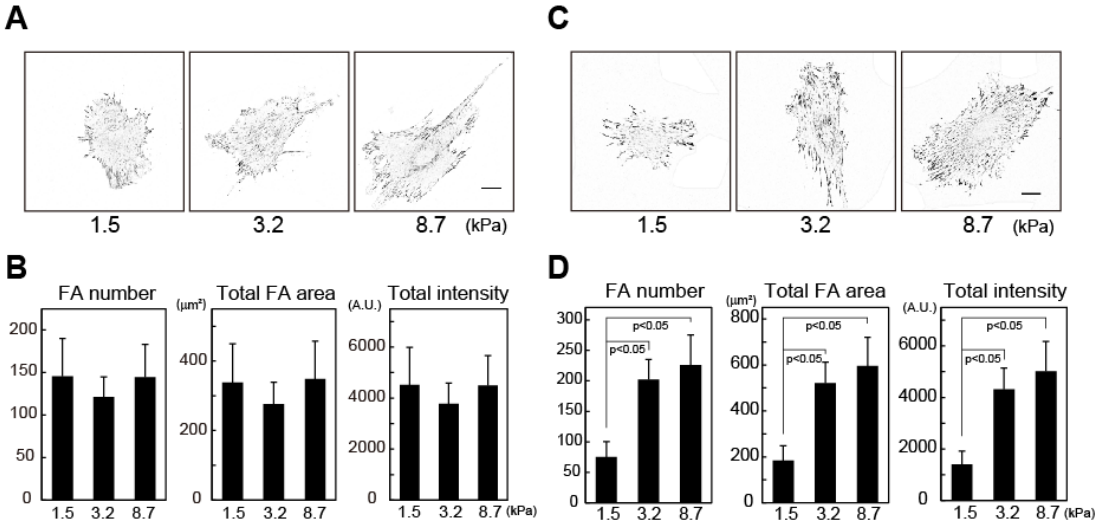

Fig. 2. ECM stiffness affected the status of vinculin. (A–D) Cells on collagen-coated substrates with various levels of stiffness (1.5 kPa, 3.2 kPa, 8.7 kPa) were fixed without (A,B) or with (C,D) CSK treatment. Cells were immunostained using anti-vinculin antibody. Images were obtained using confocal microscopy, and the gray images were inverted to increase their visibility (A,C). To obtain quantified data from single cells, neighboring cells in the images were erased. Scale bars: 20 μm. The number of FAs, total FA area and total intensity in a cell were quantified using ImageJ (B,D). More than 25 cells from two separate experiments were analyzed. Experiments were performed twice. The values represent the mean ± s.e.m. Statistical significance was determined by one-way ANOVA with Tukey's test (B,D).

stiffness. These data indicate that ECM stiffness does not affect the subcellular localization of vinculin under the author's experimental conditions. On the other hand, after treatment of cells with CSK buffer, the number and area of vinculin-containing FAs on rigid substrates were larger than those on soft substrates (Fig. 2C,D). Furthermore, the integrated intensity of CSK-resistant vinculin was also increased on rigid substrates. In addition, the plasma membrane was stained with Cell Mask Orange (Fig. 3A) to quantify the cell-spreading area and aspect ratio. No significant difference in aspect ratio among cells grown on substrates with different levels of stiffness was observed, although the cell area was slightly smaller on soft substrates (Fig. 3B). Collectively, these results suggest that ECM stiffness does not alter the subcellular localization of vinculin, but that rigid ECM increases the amount of cytoskeleton-associated vinculin in ST2 cells, similar to that observed in fibroblasts, and supports the idea that vinculin functions as a sensor for ECM stiffness in ST2 cells.

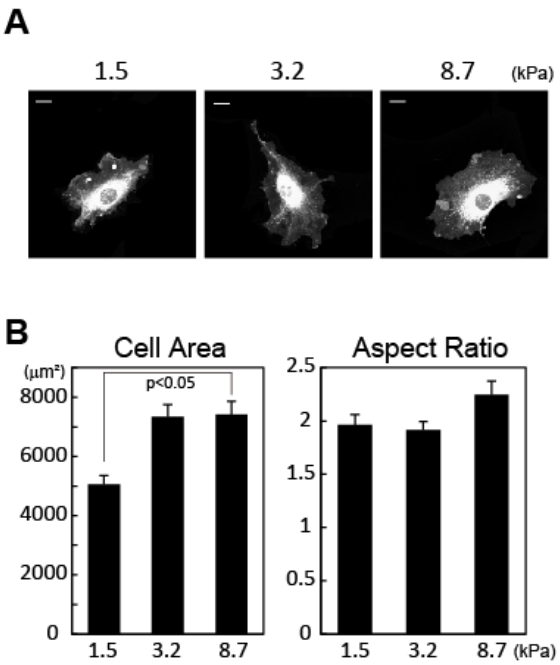

Fig. 3. The effects of vinculin-depletion on cell morphology. (A) WT ST2 cells were stained with Cell Mask Orange, and fixed. Images were obtained by confocal microscopy. (B) Cell spreading areas and aspect ratios were quantified by ImageJ from at least 30 cells from two separate experiments. The values represent the mean ± s.e.m. Statistical significance was determined by one-way ANOVA with Tukey's test (A,B).

Vinculin regulates the nuclear localization of YAP/TAZ

The transcriptional coactivators YAP and TAZ regulate the differentiation of MSCs into adipocytes and osteoblasts (3). Furthermore, ECM stiffness and contractile forces generated by the actomyosin cytoskeleton regulate the subcellular localization and activity of YAP/TAZ (6, 7). It is unknown, however, how YAP/TAZ is regulated by ECM stiffness. Therefore, the author tested whether vinculin is involved in YAP/TAZ regulation and adipocyte differentiation. First the effect of ECM stiffness on the subcellular localization of YAP/TAZ in wild-type (WT) ST2 cells was checked. Cells cultured on substrates with stiffness ranges of 1.5 kPa to 8.7 kPa in sparse conditions were immunostained with anti-YAP/TAZ antibody (Fig. 4A). The subcellular localization of YAP/TAZ was evaluated by the ratio of the intensity of YAP/TAZ signal inside the nucleus to that just outside the nucleus (nuc/cyt intensity ratio) (Fig. 4B). A larger intensity ratio indicates a stronger nuclear localization of YAP/TAZ. Consistent with previous reports (6), rigid substrates (8.7 kPa) significantly promoted the nuclear localization of YAP/TAZ compared to that seen in cells on soft substrates (Fig. 4C). These data indicate that YAP/TAZ localizes to the nucleus in an ECM stiffness-dependent manner in ST2 cells.

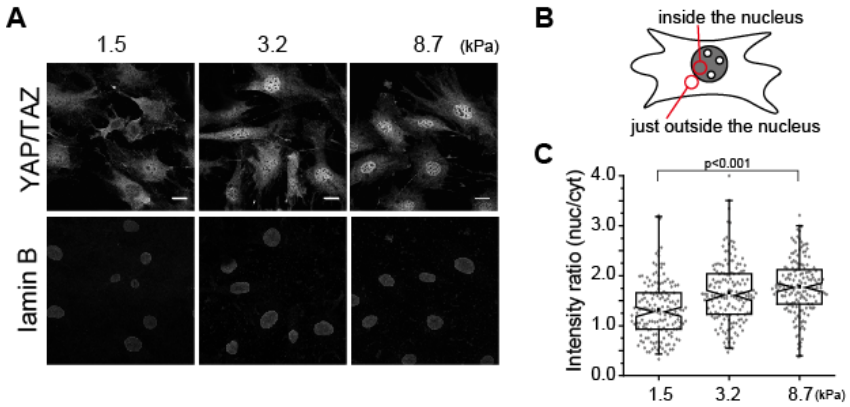

Fig. 4. The effect of ECM stiffness on YAP/TAZ nuclear localization. (A) WT cells on substrates with different levels of stiffness (1.5 kPa, 3.2 kPa, 8.7 kPa) were fixed, and YAP/TAZ and lamin B (nuclear marker) were visualized by immunostaining. Scale bars: 20 μm. (B) The ratio of nuclear-to-cytosol localization of YAP/TAZ (nuc/cyt) was determined by dividing the intensity inside the nucleus by the intensity just outside the nucleus, quantified using ImageJ. (C) The intensity ratio (nuc/cyt) of YAP/TAZ from the data shown in A was quantified. At least 150 cells from two separate experiments were analyzed. Statistical significance was determined by Kruskal–Wallis's ANOVA with Mann–Whitney's U-test.

To examine the function of vinculin in the nuclear localization of YAP/TAZ, vinculin was stably knocked down using shRNA lentivirus. Expression of vinculin was reduced to 20% in vinculin-depleted cells (Fig. 5A). Immunostaining analysis showed that the amount of vinculin localized in both cytosol and at FAs was decreased, although cytosolic vinculin was preferentially depleted (data not shown). The author first examined the effect of vinculin on the subcellular localization of YAP/TAZ on a rigid substrate. Vinculin-depleted cells and vinculin-depleted cells with re-expression of vinculin were seeded onto rigid (glass) substrates and immunostained using anti-YAP/TAZ antibody (Fig. 5B). Vinculin depletion decreased the nuc/cyt ratio of YAP/TAZ by 15 ± 4.9% (mean ± s.e.m.) compared to control cells (Fig. 5C). The re-expression of vinculin rescued the decrease (Fig. 5D). As an alternative quantification, the integrated intensity of YAP/TAZ staining in the nucleus was quantified (Fig. 5E,F). Consistent with the nuc/cyt ratio, amounts of nuclear YAP/TAZ were decreased in vinculin-depleted cells and vinculin re-expression rescued this effect. The author also performed co-immunostaining of vinculin and YAP/TAZ to investigate the correlation of the nuclear YAP/TAZ and vinculin expression at a single-cell level (Fig. 6). The integrated intensity of vinculin at FAs and that of YAP/TAZ in nuclei of individual cells were quantified (Fig. 6B). In control cells, the Spearman's correlation coefficient between vinculin and YAP/TAZ intensity was 0.66 ($P<0.001$), indicating that YAP/TAZ nuclear localization is highly correlated with vinculin localization at FAs. Vinculin depletion decreased the correlation coefficient to 0.37 ($P<0.05$). These results indicate the importance of vinculin in promoting YAP/TAZ nuclear localization.

To confirm that nuclear YAP/TAZ is transcriptionally active and promotes the expression of target genes, the mRNA expression of *Ctgf* and *Ankrd1*, major target genes, were examined by qRT-PCR. As expected, vinculin depletion decreased the relative expression of *Ctgf* and *Ankrd1* and re-expression of vinculin rescued the decrease in the expression (Fig. 5G,H).

Taken together, these data indicate that vinculin promotes the nuclear localization and activity of YAP/ TAZ on rigid substrates.

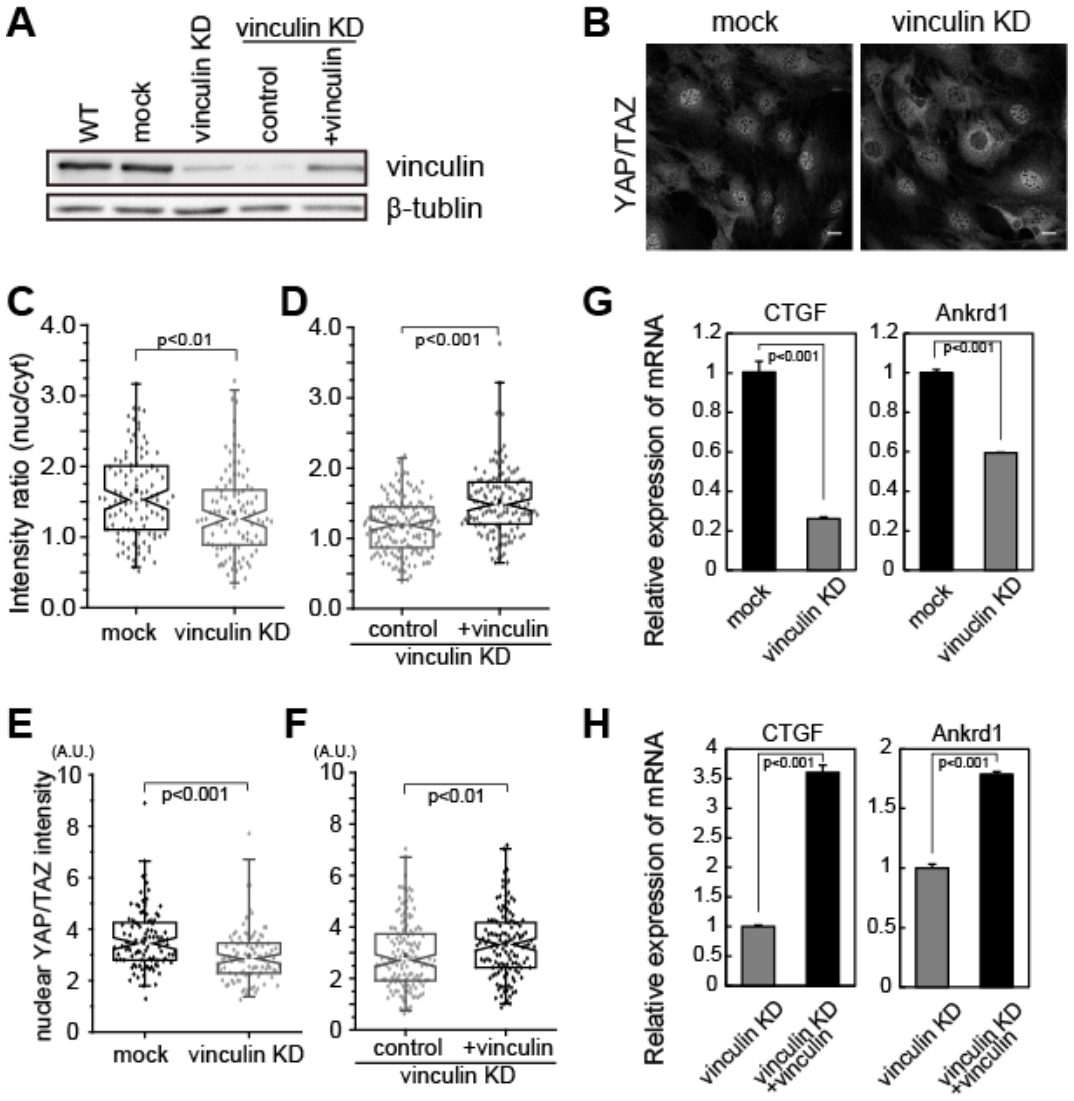

Fig. 5. Vinculin promotes the nuclear localization of YAP/TAZ on rigid ECM. (A) The expression of vinculin protein were analyzed with western-blotting. (B-D) Vinculin-depleted cells (B,C; vinculin KD) and vinculin-depleted cells re-expressing vinculin (D; vinculin KD+vinculin) on glass coated with 10 μg/ml type I collagen were fixed and immunostained using anti-YAP/TAZ antibody. At least 100 cells from two separate experiments were quantified. Experiments were performed twice. For each box plot, the box boundaries represent the 25th–75th percentiles, and the whiskers represent the 1st and 99th percentile. Notches on the box represent the confidential interval about the median value. The center dot represents the mean. (E,F) The intensity of total nuclear YAP/TAZ were quantified. (G,H) Control and vinculin-depleted cells (G) and vinculin-depleted cells re-expressing vinculin (H) were seeded on plastic dishes, and the mRNA expression of YAP/TAZ target genes were quantified by RT-PCR. The values represent the mean ± s.e.m. from triplicate experiments. Statistical significance was determined by Kruskal–Wallis's ANOVA with Mann–Whitney's U-test (C,D,E,F) or Student's t-test (G,H).

Finally, the author investigated the effects of vinculin depletion on ECM stiffness-regulated YAP/TAZ nuclear translocation. As shown in Fig. 7A,B, rigid substrates increased the nuclear localization of YAP/TAZ in control knockdown cells by 40 ± 5.6% (mean ± s.e.m.) compared to that seen on soft substrates. On the other hand, nuclear localization of YAP/TAZ was increased only moderately on rigid substrates in vinculin-depleted cells. Furthermore, the nuc/cyt intensity ratio in vinculin-depleted cells was significantly lower than in control cells on rigid substrates (8.7 kPa) (Fig. 4B). On the other hand, the distribution of YAP/TAZ on soft substrates was comparable. Hence, these data suggest that vinculin regulates the ECM stiffness-dependent subcellular localization of YAP/TAZ and promotes its nuclear localization on rigid substrates.

Actin organization mediates the vinculin-mediated enhancement of YAP/TAZ nuclear localization and activity

Nuclear localization of YAP/TAZ is suppressed by the phosphorylation of YAP/TAZ, which occurs as a result of signaling through the Hippo pathway or other pathways (12). Thus, the phosphorylation of YAP/TAZ in vinculin-depleted cells on rigid substrates was analyzed.

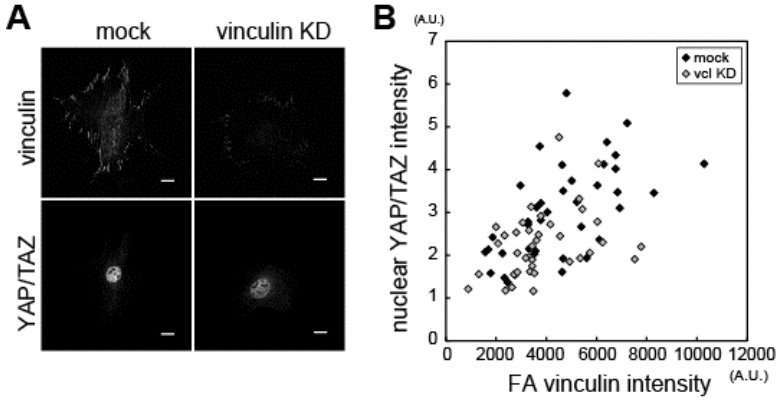

Fig. 6. YAP/TAZ nuclear localization is highly correlated with vinculin localization at FAs. (A,B) Control and vinculin-depleted cells cultured on 10 μg/ml collagen-coated cover glass were fixed with 2% paraformaldehyde for 15 min at RT, and permeabilized with 0.2% Triton X-100 containing PBS. Cells were immunostained with anti-vinculin and anti-YAP/TAZ antibody and photographed (A). Scale bars: 20 μm. Integrated density of vinculin at focal adhesions and that of YAP/TAZ in nucleus of individual cells were shown in the scatter plot (B).

Phosphorylation was slightly upregulated in vinculin-depleted cells (Fig. 8A). However, the activated (phosphorylated) form of LATS1, a YAP kinase in the Hippo pathway, was not changed between control and vinculin-depleted cells (Fig. 8A). This result suggests that vinculin does not alter the Hippo signaling pathway.

In addition to the Hippo pathway, the actin cytoskeleton is also involved in the nuclear localization and transcriptional activity of YAP/TAZ (7). Vinculin can bind to F-actin and change actin organization in other cell types (13, 14). Therefore, the author examined whether the actin cytoskeleton affects the vinculin-mediated enhancement of YAP/TAZ nuclear localization and activity. First, control or vinculin-depleted cells were cultured in the presence of cytochalasin D (cytoD), a pharmacological inhibitor of actin polymerization, and YAP/TAZ nuclear localization was investigated. Phalloidin staining indicated that the cytoD treatment disrupted the actin stress fibers in both control and vinculin-depleted cells, although there were no apparent differences between control and vinculin-depleted cells in the author's experimental conditions. The cytoD treatment suppressed YAP/TAZ nuclear localization in control cells, but hardly affected the nuclear localization of YAP/TAZ in vinculin-depleted cells (Fig. 8B,C). To evaluate the effect of

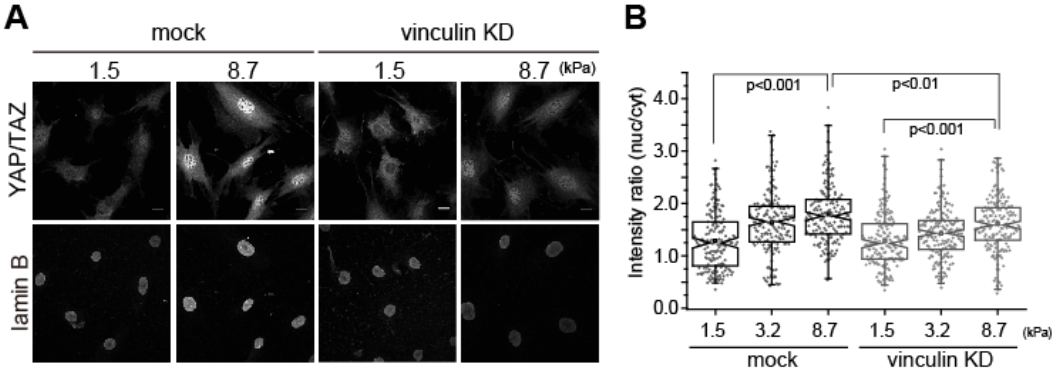

Fig. 7. Vinculin depletion attenuated the dependency of the nuclear localization of YAP/TAZ on ECM stiffness. Vinculin-depleted cells (vinculin KD; 7.5×10^4 cells/35 mm dish) were seeded on collagen-coated substrates with different levels of stiffness (1.5 kPa, 3.2 kPa, 8.7 kPa) and immunostained using anti-YAP/TAZ antibody. Scale bars: 20 μm. (B) The intensity ratios (nuc/cyt) of YAP/TAZ was quantified for at least 170 cells from three separate experiments as shown in A. For each box plot, the box boundaries represent the 25th–75th percentiles, and the whiskers represent the 1st and 99th percentile. Notches on the box represent the confidential interval about the median value. The center dot represents the mean. Statistical significance was determined by Kruskal–Wallis ANOVA with Mann–Whitney's U-test.

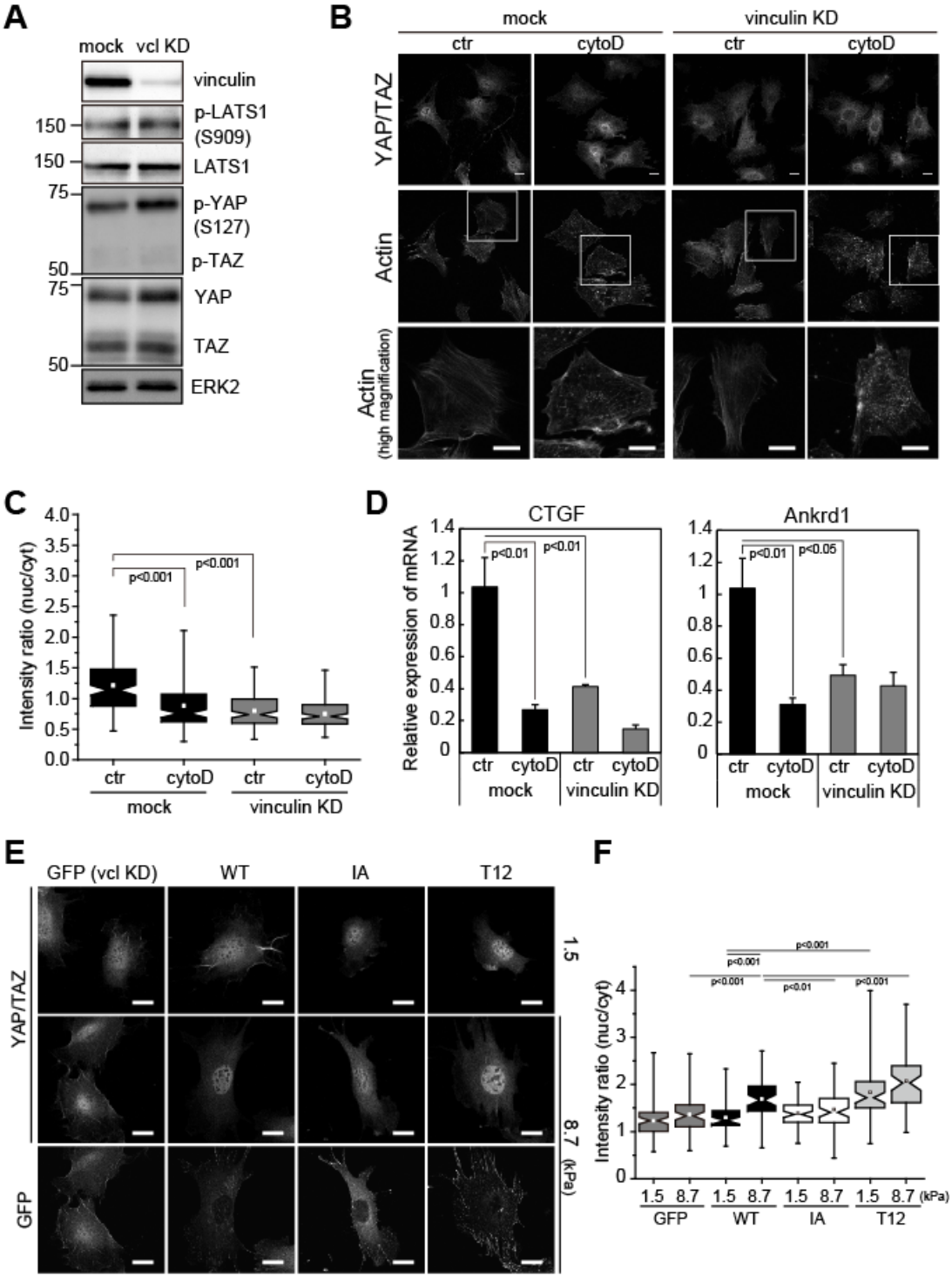

Fig. 8. Vinculin promoted nuclear localization and activity of YAP/TAZ through the F-actin organization. (A) Equal amount of cell lysates were analyzed by western blotting with indicated antibodies. ERK2 serves as a loading controls. Results were representative of triplicate experiment. (B)Vinculin-depleted cells (vinculin KD) on glass coated with 10 μg/ml type I collagen were treated with 1 μM cytochalasin D for 6 h. Cells were fixed and immunostained using anti-YAP/TAZ and Alexa-Fluor-568–phalloidin. Scale bars: 20 μm. (C) The intensity ratios (nuc/cyt) of YAP/TAZ was quantified for at least 100 cells from two separate experiments as shown in B. (→continue to the next page below)

cytoD in transcriptional activity of YAP/TAZ, the relative expression of *Ctgf* and *Ankrd1* mRNA was examined (Fig. 8D). As expected, cytoD treatment decreased the expression of Ctgf and Ankrd1 mRNA by up to 30% compared to vehicle in control cells. Vinculin depletion abrogated the decrease in the *Ctgf* and *Ankrd1* expression induced by the cytoD treatment. Taken together, these results suggest that the vinculin-mediated enhancement of YAP/TAZ nuclear localization and activity involves actin organization.

To further gain insight into the relation between actin organization and vinculin, we used the vinculin mutants I997A (denoted IA, deficient in actin binding) and T12 (constitutively active (open form)) (15, 16). GFP-fused vinculin mutants were expressed in ST2 vinculin-depleted cells. Then, the proportion of YAP/TAZ that showed nuclear localization in these cells on PAA substrates was evaluated. In vinculin-depleted cells re-expressing WT vinculin, YAP/TAZ nuclear localization was increased by 30 ± 5.9% (mean ± s.e.m.) on rigid substrates (8.7 kPa) compared to on soft substrates (1.5 kPa), and showed ECM stiffness-dependent YAP/TAZ nuclear localization (Fig. 8E,F). On the other hand, in vinculin-depleted cells re-expressing IA vinculin, the YAP/ TAZ nuclear localization was lower than that in WT-re-expressing cells on rigid substrates (8.7 kPa) and no significant difference was observed between soft and rigid substrates. In contrast, the YAP/TAZ nuclear localization in vinculin-depleted cells re-expressing T12 vinculin was high even on soft substrate (1.5 kPa). Much higher nuclear localization was observed on rigid substrates (8.7 kPa) in these T12-expressing cells compared to

---

Fig. 8. (D) Vinculin-depleted cells on plastic dishes were treated with 1 μM cytochalasin D for 24 h. The mRNAs were extracted, and expression of *Ctgf* and *Ankrd1* was quantified by qRT-PCR. The values represent the mean ± s.e.m. for triplicate experiments. (E) Vinculin-depleted cells re-expressing vinculin (WT, IA or T12) were cultured on collagen-coated substrates with different levels of stiffness (1.5 kPa and 8.7 kPa) and immunostained using anti-YAP/TAZ antibody. GFP indicates no re-expression. (F) Intensity ratios (nuc/cyt) of YAP/TAZ in at least 60 cells from two separate experiments as shown in D were quantified. For each box plot, the box boundaries represent the 25th–75th percentiles, and the whiskers represent the 1st and 99th percentile. Notches on the box represent the confidential interval about the median value. The center dot represents the mean. Statistical significance was determined by Kruskal–Wallis ANOVA with Mann–Whitney's U-test (C,F) or one-way ANOVA with Tukey's test (D).

both that on soft substrates for T12-expressing cells and that on rigid substrates for WT vinculin-expressing cells. These results strongly suggest that actin binding of vinculin is involved in the regulation of YAP/TAZ.

Vinculin regulates ECM stiffness-dependent adipocyte differentiation

The author next investigated the effects of vinculin on the differentiation into adipocytes. First, the author tested the differentiation of vinculin-depleted cells into adipocytes on rigid (plastic) substrates. Quantitative qRT-PCR analysis showed that vinculin depletion markedly increased the expression of mRNA encoding PPARγ2 and aP2 (Fig. 9A). Western blotting showed an increased expression of aP2 protein in vinculin-depleted cells (Fig. 9B). The differentiation was further assessed by measuring the accumulation of lipid droplets using Oil Red O staining. Vinculin-depleted cells contained more lipid droplets than control cells (Fig. 9

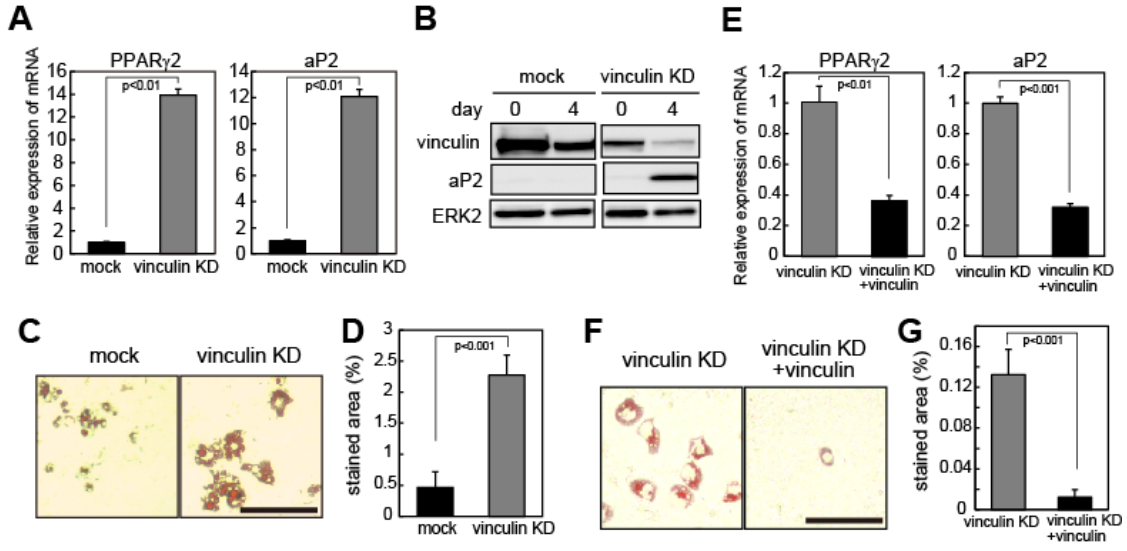

Fig. 9. Vinculin suppressed the differentiation into adipocytes on rigid substrate. Vinculin-depleted cells (vinculin KD; A–D) and vinculin-depleted cells re-expressing vinculin (vinculin KD+vinculin; E–G) were seeded on plastic dishes and differentiated into adipocytes. (A,E) On day 6 after MDI treatment, mRNAs were extracted, and expression of mRNAs encoding PPARγ2 and aP2 was quantified by qRT-PCR from triplicate experiments. (B) Equal amounts of total cell lysates collected on day 4 were analyzed by western blotting using the indicated antibodies. (C,D,F,G) Cells were stained with Oil Red O on day 6 after MDI treatment. Scale bar: 200 μm. (D,G) Nine images were obtained from three independent experiments, and the percentage of area stained was determined with ImageJ and shown in the graphs. The values represent the mean ± s.e.m. All experiments were performed twice. Statistical significance was determined by Student's t-test (A,D,E,G).

C,D). These data suggest that vinculin depletion promotes the adipocyte differentiation on rigid substrates. To confirm the effects of vinculin depletion on the differentiation into adipocytes, vinculin-depleted cells re-expressing vinculin were induced to differentiate into adipocytes on rigid (plastic) substrates. Expression of mRNA encoding PPARγ2 and aP2 was lower in vinculin re-expressing cells than in vinculin-depleted cells (Fig. 9E), and the amount of lipid droplets was smaller than in vinculin-depleted cells (Fig. 9F,G). These results indicate that vinculin suppresses adipocyte differentiation on rigid substrates.

To check whether vinculin also affects the differentiation into osteoblasts on rigid substrates, ALP mRNA expression was quantified. Vinculin depletion significantly decreased the mRNA expression of ALP (Fig. 10A), and vinculin re-expression rescued this decrease (Fig. 10B). The author also checked the ALP activity by ALP activity staining. Quantified data showed that Vinculin-depletion decreased ALP activity (Fig. 10C). Taken together, these observations indicate that vinculin regulates the balance between adipogenic and osteogenic lineage commitment.

The author next investigated the effect of vinculin depletion on ECM stiffness-dependent adipocyte differentiation. Vinculin-depleted cells were cultured on PAA substrates and induced to differentiate into adipocytes. Expression of mRNA encoding PPARγ2 and aP2

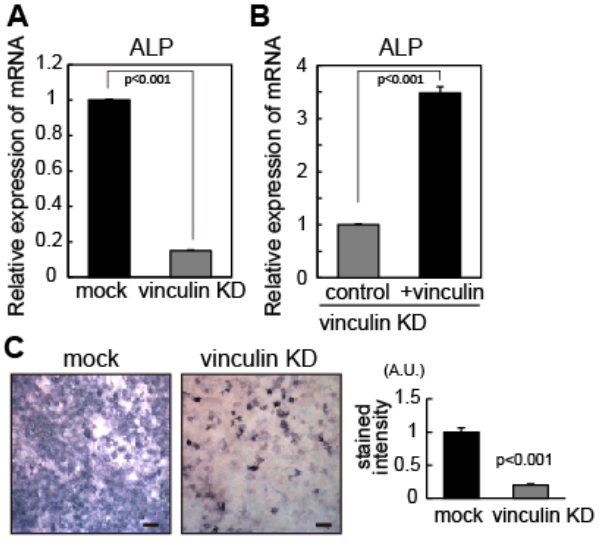

Fig. 10. Vinculin promotes osteoblast differentiation on rigid substrates. Vinculin-depleted cells (A,C) and vinculin re-expressing cells (B) were seeded on plastic dishes and cultured as described in Fig.1C. (A,B) On the sixth day after seeding, mRNA expression of ALP were quantified by qRT-PCR. (C) ALP activity staining assay were performed and integrated intensity were quantified by Image J. Scale bars represent 400 μm. Statistical significance were tested by Student's T-test.

expression was 2-fold lower on rigid substrates (8.7 kPa) than those on soft substrates (1.5 kPa) in control cells, as with the WT ST2 cells, indicating an ECM stiffness-dependent differentiation (Fig. 11A). By contrast, although vinculin depletion led to a 2-4 -fold increase in adipocyte differentiation compared with control cells on soft substrates, there was no significant difference in the expression of adipogenic markers between vinculin-depleted cells cultured on soft and rigid substrates (Fig. 11A). Stiffness-dependent differentiation was further investigated by Oil Red O staining (Fig. 11B). In control knockdown cells, the area stained by Oil Red O on soft substrates (1.5 kPa) was 3.0 ±0.85-fold larger than that on rigid substrates (8.7 kPa). On the other hand, the stained area was not changed by ECM stiffness in vinculin-depleted cells (Fig. 11C). Taken together, these results suggest that vinculin depletion attenuates the ECM-stiffness dependency of adipocyte differentiation.

Because the author found that association of vinculin with actin is involved in regulation of YAP/TAZ nuclear localization, the author examined the role of this association in adipocyte differentiation. Vinculin-depleted cells re-expressing WT or IA vinculin were cultured on rigid (plastic) substrates. Whereas re-expression of WT vinculin reduced expression of mRNA encoding PPARγ2 and aP2 to 25 ± 1.8% (PPARγ2) or 28 ± 1.3% (aP2), re-expression of IA vinculin only reduced these to 82 ± 8.2% (PPARγ2) or 82 ± 7.5% (aP2) (mean ± s.e.m.; Fig. 11D). This result suggests that IA vinculin inhibits adipocyte differentiation less efficiently than WT vinculin. Oil Red O staining also confirmed the weak effect of IA vinculin on adipocyte differentiation (Fig. 11E,F). Collectively, these observations suggest that vinculin regulates ECM stiffness-dependent adipocyte differentiation through its association with actin.

Interaction of vinculin with vinexin α is involved in ECM stiffness-dependent cell migration in mouse embryonic fibroblasts (11). Thus, the author also examined the effect of vinexin depletion on differentiation into adipocytes, but did not detect any increase in

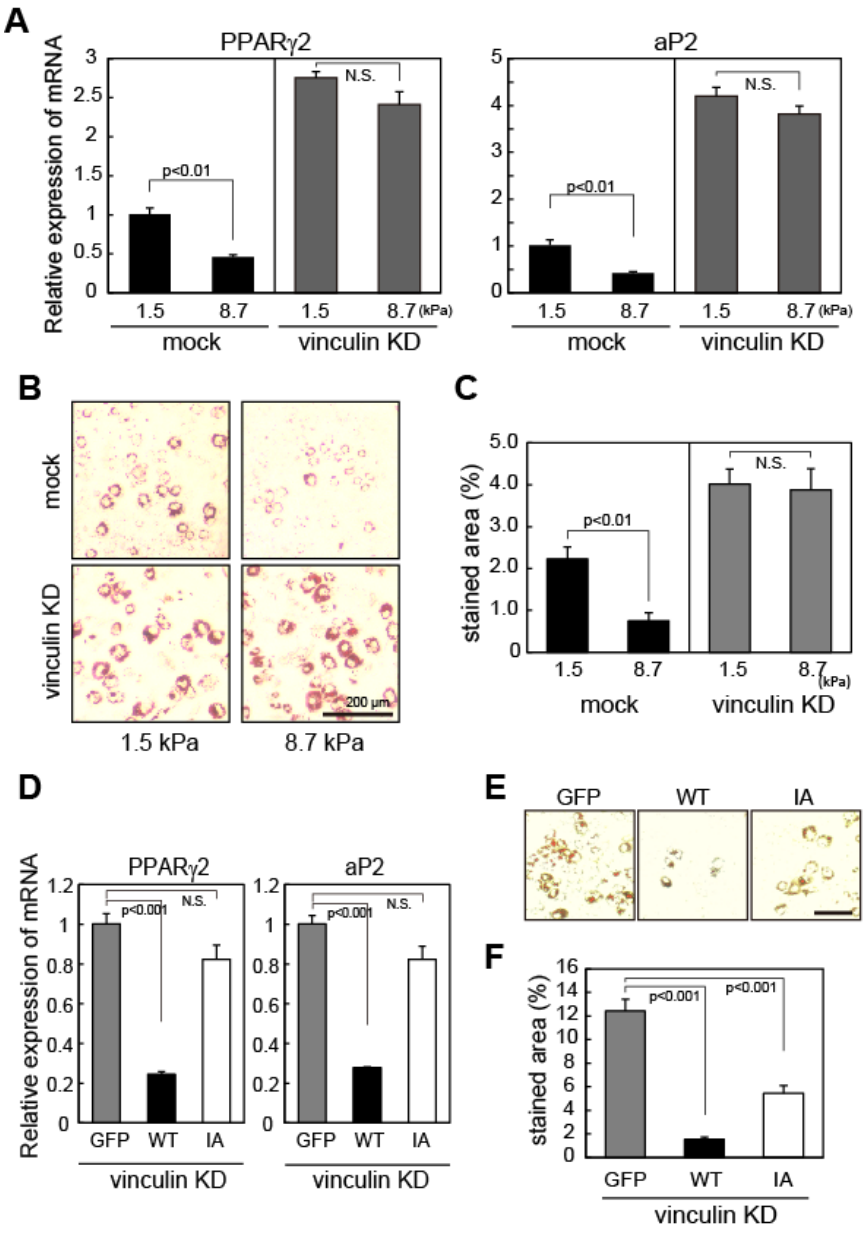

Fig. 11. Vinculin depletion attenuated the ECM stiffness-dependency of the differentiation into adipocyte. (A–C) Control or vinculin-depleted (vinculin KD) cells on collagen-coated substrates with different levels of stiffness (1.5 kPa, 8.7 kPa) were differentiated into adipocytes as in Fig. 1A. (A) On day 6 after MDI treatment, mRNA were extracted and expression of adipogenic markers was quantified by qRT-PCR from triplicate experiments. Experiments were performed three times. (B,C) Cells were stained with Oil Red O on day 6 after MDI treatment. Scale bar: 200 μm. (C) At least six images were obtained from two independent experiments, and the percentage of area stained was determined with ImageJ and shown in the graphs. (D–F) Vinculin-depleted cells re-expressing vinculin (WT or IA) were seeded on plastic dishes and differentiated into adipocytes. GFP indicates no re-expression. (D) On day 6 after MDI treatment, mRNAs were extracted, and expression of mRNA encoding PPARγ2 and aP2 was quantified by qRT-PCR from triplicate experiments. Relative expression compared to that in control cells is shown. (E,F) Cells were stained with Oil Red O on day 6 after MDI treatment. Scale bar: 200 μm. (F) Nine images were obtained from three independent experiments, and the percentage of area stained was determined with ImageJ and shown in the graphs. The values represent the mean±s.e.m. Statistical significance was determined by Student's t-test (A,C) or one-way ANOVA with Tukey's test (D,F). N.S., not significant.

differentiation (data not shown), possibly due to other functions of vinexin such as regulating signal molecules. To assess this possibility further, the author used P2 mutant vinculin, which has a reduced affinity to vinexin (11). To check whether the P2 mutation affects vinculin activation in ST2 cells, the author first examined the resistance of vinculin to CSK treatment on rigid substrates (8.7 kPa) (Fig. 12A-C). Consistent with previous work (11), the P2 mutation decreased

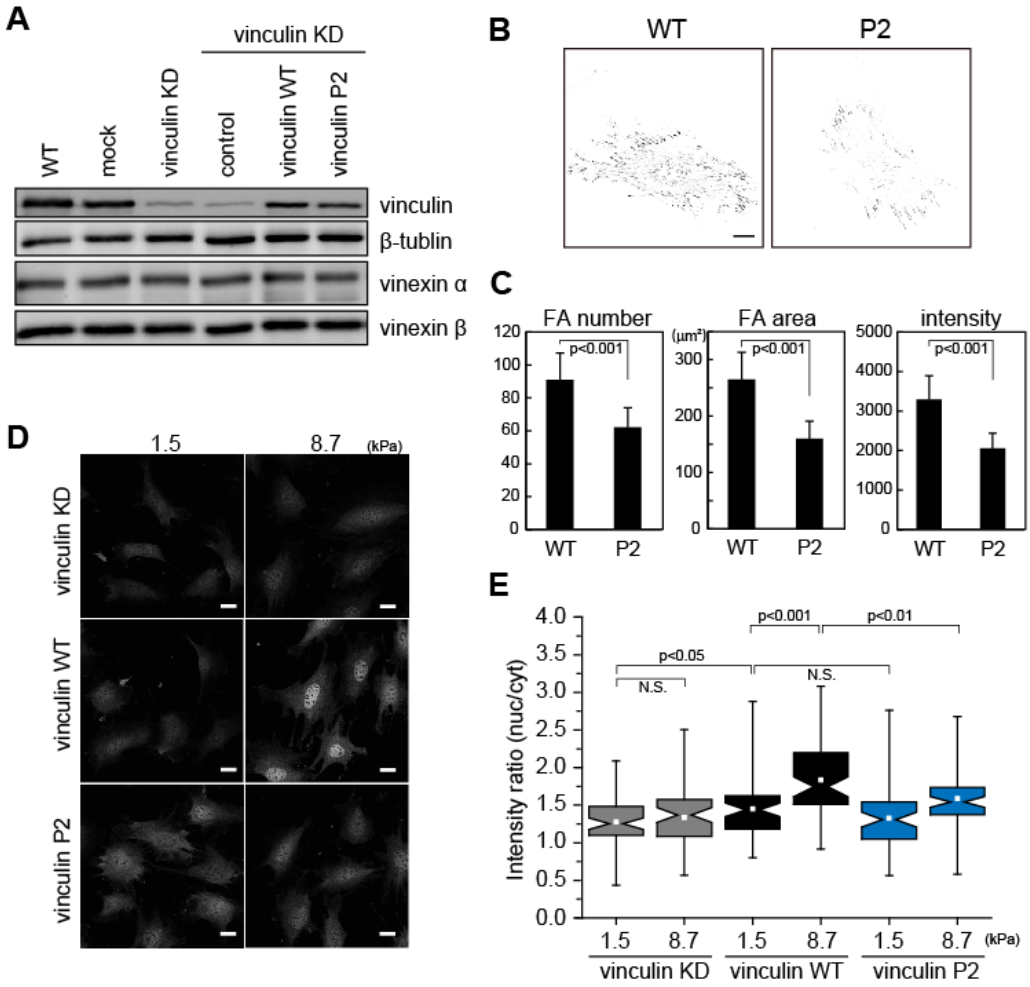

Fig. 12. P2 mutation of vinculin affects the nuclear localization of YAP/TAZ. (A) WT and P2 vinculin re-expressing cells were lysed with 1% SDS and equal amount of total lysates were analyzed with western blotting. 'mock' and 'control' represent pLKO.1 vector-transfected cells and pCDH vector-transfected vinculin-depleted cells, respectively. (B,C) WT and P2 vinculin re-expressing cells were seeded on collagen-coated substrates (8.7 kPa) and CSK buffer resistant vinculin were analyzed. (D,E) WT and P2 vinculin re-expressing cells were seeded on collagen-coated substrates (1.5 kPa and 8.7 kPa) and immunostained as described in Fig. 4A. More than 25 cells (C) or 55 cells (E) from two separate experiments were analyzed. Scale bars represent 20 μm. Statistical significance was determined by Student's T-test (C) or Kruskal Wallis ANOVA, Mann-Whitney's U-test (E).

the amount of CSK-resistant vinculin (the vinculin-positive FA number, area and intensity) compared to that seen with WT vinculin (Fig. 12C). Next, to test whether the P2 mutation affects ECM stiffness-dependent YAP/TAZ nuclear localization, WT and P2 vinculin-expressing cells cultured on PAA substrates were analyzed by immunostaining (Fig. 12D,E). Rigid substrates increased YAP/TAZ nuclear localization by 30 ± 6.3% compared to that seen on soft substrates for WT vinculin-expressing cells. On the other hand, rigid substrates increased the localization only moderately (20 ± 6.3%) in P2-vinculin expressing cells. Furthermore, YAP/TAZ nuclear localization on rigid substrates in P2 vinculin expressing cells was significantly lower than that on rigid substrates in WT vinculin- expressing cells. Although the author also investigated the effect of P2 mutation on adipocyte differentiation, this mutation did not affect the mRNA expression of adipogenic markers either on substrates with different levels of stiffness or on extremely rigid plastic dishes (data not shown), suggesting that the moderate effect of the P2 mutation on YAP/TAZ localization is not enough for the regulation of adipocyte differentiation. Taken together, these results suggest that vinculin–vinexin interaction is involved in regulating YAP/TAZ nuclear localization.

Regulation of YAP/TAZ activity and adipocyte differentiation via vinculin is conserved in human MSCs

To examine whether the role of vinculin in YAP/TAZ regulation and adipocyte differentiation is shared among MSCs, the author also tested the effect of vinculin depletion using UE7T-13 cells, a human MSC cell line (17). Vinculin-depleted cells were established using shRNA. First, the author checked the effect of vinculin depletion on the YAP/TAZ transcriptional activity. Vinculin-depleted human MSCs showed lower mRNA expression of YAP/TAZ target genes, e.g. CTGF and ANKRD1 (Fig. 13A). Next, the author examined the effect on the adipocyte

differentiation. The vinculin-depleted human MSCs were induced to differentiate into adipocytes. The mRNA expression of adipogenic markers was investigated. The author found that the expression of mRNA encoding PPARγ2 and aP2 in vinculin-depleted adipocytes was significantly higher than in control cells (Fig. 13B). Furthermore, depletion of vinculin through transient transfection of small interfering (si)RNAs directed against human vinculin into UE7T-13 cells upregulated both mRNA and protein expression of aP2 in siRNA-transfected cells (data not shown). These results suggest that vinculin-mediated regulation of YAP/TAZ activity and suppression of adipocyte differentiation is not limited to ST2 cells but is a shared property of MSCs.

TAZ mediates the effect of vinculin on adipocyte differentiation

To examine whether YAP or TAZ was responsible for suppression of differentiation into adipocytes by vinculin, siRNAs targeted against YAP or TAZ were transfected into control and vinculin-depleted cells and the effect of YAP or TAZ knockdown on the adipocyte differentiation was examined. Because combinatorial treatment of YAP or TAZ knockdown with adipogenic stimulation (IBMX, insulin and dexamethasone) severely damaged ST2 cells under the author's conditions, the effect of YAP or TAZ knockdown on the differentiation without

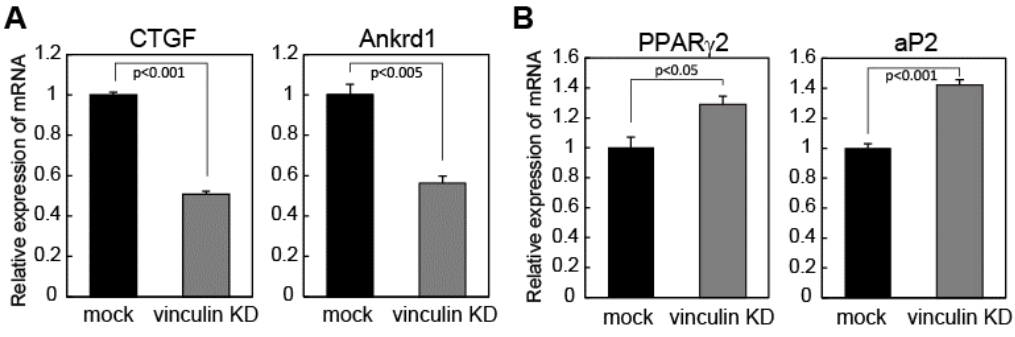

Fig. 13. Regulation of YAP/TAZ activity and adipocyte differentiation via vinculin is conserved in human MSCs. (A) Vinculin-depleted UE7T-13 cells were seeded on plastic dishes, and mRNA expression of CTGF and Ankrd1 was quantified by q RT-PCR. (B) Vinculin-depleted UE7T-13 cells were differentiated into adipocytes by changing MDI containing medium every 2 days. On the sixth day, RNAs were extracted, and adipogenic marker expression was quantified by qRT-PCR.

adipogenic stimulation was examined. Under this condition, cells still differentiate into adipocytes although the efficiency is moderate. Although YAP siRNA transfection efficiently reduced the expression of YAP, YAP knockdown only slightly affected the expression of both PPARγ2 and aP2 in WT ST2 cells (Fig. 14A). Transfection of siRNAs against TAZ efficiently reduced the TAZ expression (Fig. 14B). Knockdown of TAZ increased the expression of aP2-encoding mRNAs to 2.6 ± 0.15-fold (siRNA#1) or 1.7 ± 0.15-fold (siRNA#2) in control cells, whereas knockdown of TAZ slightly increased the expression [1.7 ± 0.08-fold (siRNA#1) or 1.1 ± 0.05-fold (siRNA#2)] in vinculin-depleted cells (mean ± s.e.m.; Fig. 14C). PPARγ2 expression was also increased efficiently by TAZ knockdown in control cells [2.2 ± 0.05-fold (siRNA#1) or 1.6 ± 0.05-fold (siRNA#2)] and moderately in vinculin-depleted cells [1.7 ± 0.03-fold (siRNA#1) or 1.3 ± 0.002-fold (siRNA#2)]. These results indicate that TAZ knockdown is less effective in vinculin-depleted cells because vinculin depletion already suppresses TAZ nuclear localization and activity. To further analyze this effect, the author also transfected TAZ siRNA in combination with YAP siRNA. Similar to the results with TAZ knockdown alone, simultaneous knockdown of YAP and TAZ increased the level of mRNAs encoding PPARγ2 and aP2 in control cells, whereas knockdown of YAP and TAZ only slightly affected this in vinculin-depleted cells (Fig. 14D,E). Taken together, these results indicated that TAZ, at least partially, inhibits adipocyte differentiation downstream of vinculin.

DISCUSSION

Physical properties of the extracellular microenvironment have emerged as an important factor controlling the differentiation of stem cells. ECM stiffness can direct the lineage commitment of MSCs. They differentiate into neuroblasts or adipocytes on soft ECM and into osteoblasts on rigid ECM (18). The transcriptional coactivators YAP and TAZ are known as

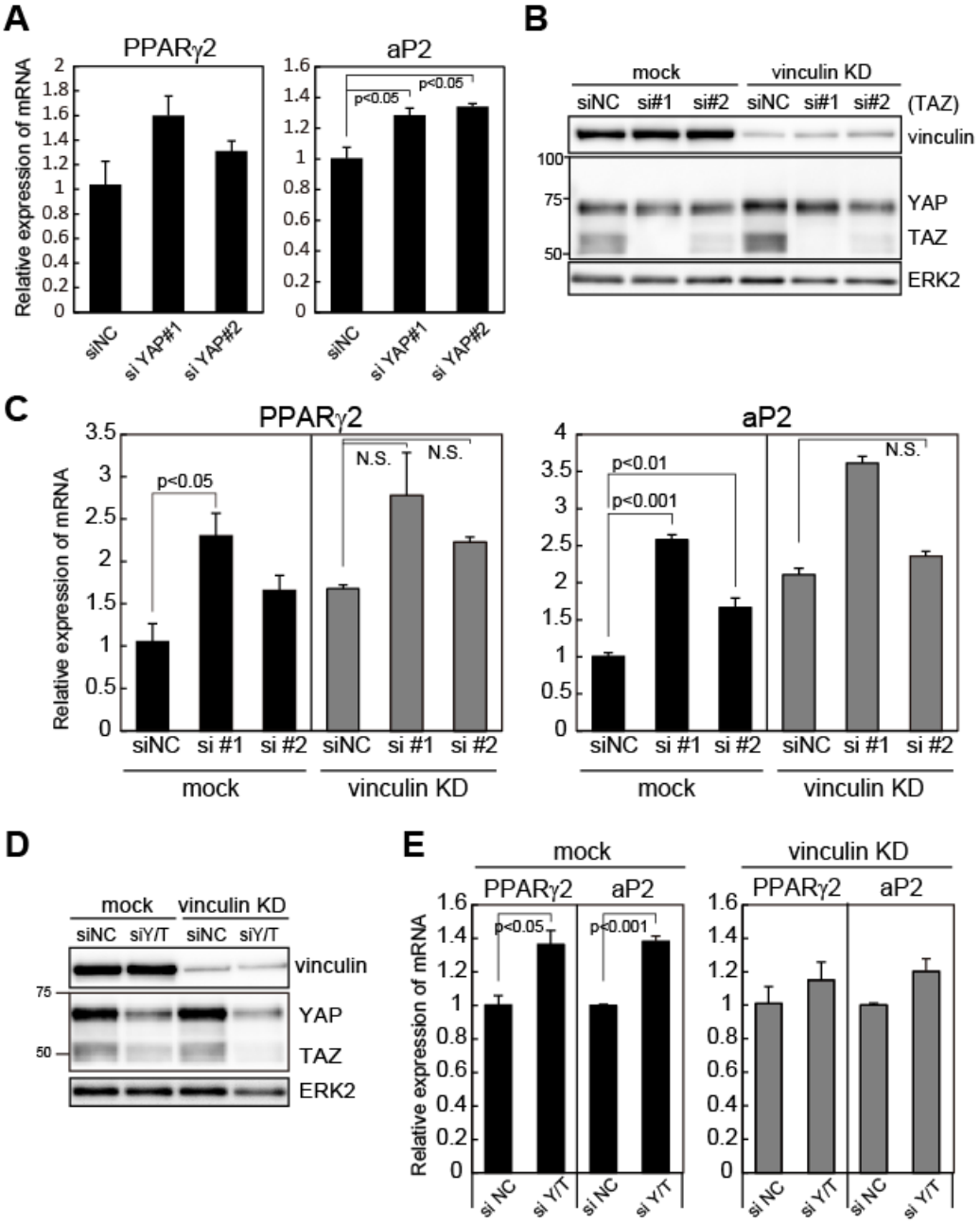

Fig. 14. Effect of YAP/TAZ knockdown on the adipocyte differentiation of vinculin-depleted cells. (A) WT ST2 cells were transfected with negative control (siNC) or YAP-targeted siRNA (#1,#2). mRNA expression of adipogenic markers was quantified by qRT-PCR. (B,C) WT and vinculin depleted cells (vinculin KD) were transfected with negative control (siNC) or TAZ-targeted siRNA (si#1, si#2) using RNAiMAX. (B) TAZ expression was analyzed by western blotting. (C) On day 6 after siRNA transfection, the expression of mRNA encoding PPARγ2 and aP2 were quantified by qRT-PCR and normalized to GAPDH expression. The relative expression to that with negative control siRNA in control cells is shown in the graph. (D,E) Vinculin-depleted cells were transfected with 0.5 nM YAP-targeted siRNA(#2) and 1.5 nM TAZ targeted siRNA(#2). (E) The expression of mRNA encoding PPARγ2 and aP2 were quantified by qRT-PCR and normalized to GAPDH expression. The relative expression to that with negative control siRNA in control cells is shown in the graph. The values represent the mean ± s.e.m. from triplicate experiments. Statistical significance was determined by one-way ANOVA with Tukey's test. N.S., not significant.

mediators of mechanical signals; however, how ECM stiffness regulates lineage specification and which molecules are involved in the YAP/TAZ regulation remain unclear. Here, the author showed that rigid ECM suppressed the differentiation of ST2 mesenchymal cells into adipocytes and promoted the differentiation into osteoblasts. Vinculin status, estimated by its resistance to CSK treatment, was regulated by ECM stiffness. Vinculin promoted the nuclear localization and activity of YAP/TAZ on rigid substrates, and suppressed the adipocyte differentiation and promoted osteoblast differentiation on rigid ECM. Furthermore, vinculin depletion attenuated the ECM stiffness-dependent nuclear localization of YAP/TAZ and adipocyte differentiation. Collectively, these observations indicate that vinculin functions as a sensor for ECM stiffness and regulates the differentiation of MSCs via promoting the nuclear localization of YAP/TAZ.

During adipocyte differentiation both *in vitro* and *in vivo*, the type and density of ECM components dramatically change. These changes lead to the alteration of cell morphology and cytoskeletal organization, and affect the differentiation through FAs. Although some studies have focused on the involvement of signaling molecules localized at FAs, including FAK (also known as PTK2), in adipocyte differentiation (19-21), the functions of cytoskeletal FA proteins such as talin and vinculin in adipogenesis have not been studied. Here, the author's observations showed that vinculin suppressed the differentiation into adipocytes and promoted differentiation into osteoblasts on rigid ECM. To the author's knowledge, the present study is the first study that sheds light on the FA scaffold protein vinculin as a regulator of adipocyte differentiation.

The author identified here a novel role for vinculin as a regulator of YAP/TAZ in MSCs. Vinculin promoted the nuclear localization and activity of YAP/TAZ on rigid substrates. Although the Hippo signaling pathway is known to regulate the localization and activity of YAP/TAZ to mediate the contact inhibition of cell proliferation and the control of organ size (22, 23), the phosphorylation of LATS1, a YAP kinase in the Hippo pathway, was not affected by

vinculin in the present study. This is consistent with a previous report showing that ECM stiffness-dependent YAP/TAZ regulation is independent of LATS1 phosphorylation (6). Importantly, vinculin depletion did not affect the localization and activity of YAP/TAZ under F-actin-disrupted conditions, indicating that actin organization is essential for the vinculin-mediated regulation of YAP/TAZ. The requirement of proper actin organization for mechanical regulation of YAP/TAZ has also been reported by others. Stress fiber formation is an important factor in cell morphology- and ECM stiffness-directed YAP/TAZ regulation (6, 7). Furthermore, Aragona et al. showed that knockdown of the F-actin capping or severing proteins CapZ, cofilin and gelsolin, increases F-actin bundling and promotes the nuclear localization of YAP/TAZ on soft ECM (4). Interestingly, vinculin directly binds to F-actin (24, 25) and has F-actin-bundling and -capping activities (14, 26). Here, the author demonstrated that actin-binding deficient vinculin I997A (15) lacks the ability to promote the change in the YAP/TAZ nuclear localization that is dependent on ECM stiffness. Taken together, these observations indicate that vinculin regulates YAP/TAZ at least partly through organization of actin cytoskeleton.

Here, the author showed that vinculin status, as estimated by the resistance to CSK treatment, was regulated by ECM stiffness in ST2 MSCs, and that ECM stiffness-dependent differentiation required vinculin expression. The author also demonstrated that mutation of the vinexin-binding site in vinculin reduced the ability of vinculin to promote YAP/TAZ nuclear localization. The author's group previously revealed that the interaction of vinculin with vinexin α functions as a mechanosensor for ECM stiffness, and this interaction is a prerequisite for the stiffness-dependent regulation of vinculin status and cell migration in mouse embryonic fibroblasts (11). In agreement with the author's findings, Holle et al. reported that vinculin and vinexin have an essential role in myogenic differentiation (27). Thus, the present study extends the understanding of the vinculin function in mechanosensing and mechanotransduction to the

regulation of cell differentiation and to MSCs.

In addition to the function of vinculin as a sensor of ECM stiffness, vinculin also can sense other physical microenvironments. Janoštiak et al. have also reported that vinculin binding to p130CAS serves as a sensor for stretch and regulates the stretch-induced activation of p130CAS (28). Grashoff et al. reported the requirement of tension to activate vinculin (29). Vinculin binding to talin at FAs occurs under force-generating conditions (30). Taken together, these observations suggest that vinculin is used as a 'mechanosensor' for various physical cues.

Another important finding in this study is that vinculin determines the lineage commitment of ST2 mesenchymal stem cells. Rigid ECM promotes the nuclear localization of YAP/TAZ and osteogenesis but suppresses adipogenesis (6, 8). TAZ regulates the balance between adipogenesis and osteogenesis (3). Here, the author showed that vinculin promotes expression of the osteogenic gene, ALP, while it inhibits the differentiation into adipocytes. Furthermore, knockdown of TAZ by siRNA dampened the vinculin-mediated suppression of differentiation into adipocytes on rigid ECM. Recent reports have also shown that vinculin can regulate myogenesis (10) and chondrogenesis (31) in a stiffness-dependent or -independent manner, respectively. Taken together, these results show that vinculin has a significant role in mesenchymal lineage commitment.

The author demonstrated that vinculin promotes the activity of YAP/TAZ. YAP/TAZ is notable for its role in cancer progression. YAP has oncogenic potential, leading to epithelial-to-mesenchymal transition and cell proliferation in breast cancer (32-34). While cancer tissues have more rigid ECM than with normal tissues, YAP is activated and contributes to ECM stiffening in cancer-associated fibroblasts (35). Vinculin is also involved in metastasis and malignancy of various cancers, including pancreatic, prostate and breast cancers (36-38). The author's results indicate that vinculin could regulate tumor progression through YAP/TAZ, in addition to through

signals already known to be involved in tumorigenesis.

Elosegui-Artola et al. have recently reported that talin regulates YAP/TAZ nuclear localization on substrates above 11 kPa, in accordance with the talin-unfolding state in mouse embryonic fibroblasts (39). They also showed that expression of the vinculin head domain, which could work as a dominant-negative mutant, suppressed the effect of talin. The present study demonstrated that vinculin modulated the ECM stiffness-dependent YAP/TAZ nuclear localization on substrates between 1.5 kPa and 8.7 kPa in ST2 mesenchymal stem cells. Under this condition, ECM stiffness did not affect the subcellular localization of vinculin at FAs but increased the amount of activated and cytoskeleton-associated vinculin. These observations suggest that vinculin could work as a mechanosensor in at least two fashions: one through detecting the talin unfolding on substrates above 11 kPa and the other through modulating vinculin activation on substrates between 1.5–8.7 kPa independently of talin unfolding. Alternatively, vinculin could work as a mechanosensor at different ranges of stiffness in different cellular contexts. Taken together, these observations indicate that ECM stiffness-dependent YAP/TAZ nuclear localization involves FA mechanosensitive proteins, including talin and vinculin.

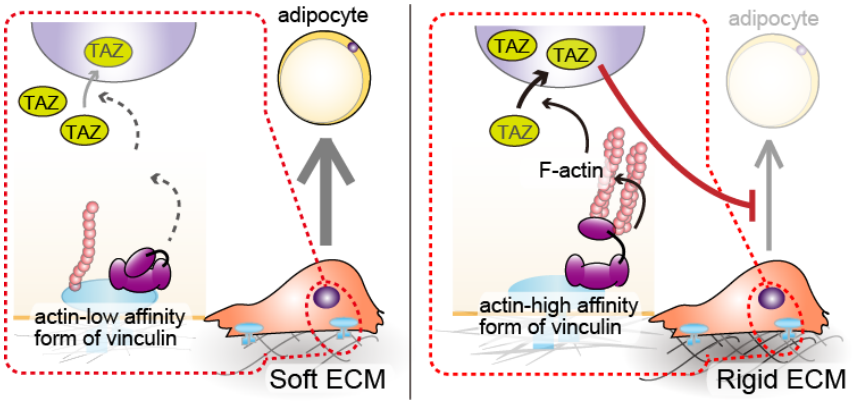

Fig. 15. A schematic model of ECM stiffness dependent differentiation by vinculin. On soft ECM, the vinculin head-tail interaction inhibits the association of F-actin at FAs. TAZ remains in the cytosol and does not inhibit adipocyte differentiation (left). On rigid ECM, vinculin changes its conformation to actin-high affinity form, as can be estimated by its resistant to CSK treatment. Vinculin promotes TAZ nuclear translocation via the actin cytoskeleton and suppresses adipocyte differentiation.

In summary, the author demonstrated that vinculin promotes the ECM stiffness-dependent nuclear localization of YAP/TAZ and suppresses adipocyte differentiation in a manner that depends on ECM stiffness. The effect of TAZ knockdown on adipocyte differentiation was less effective in vinculin-depleted cells than in control cells. Thus, the author proposes a model, in which vinculin senses ECM stiffness and regulates differentiation through promoting the nuclear localization of TAZ (Fig. 15).

MATERIALS AND METHODS

Antibodies and reagents

Mouse anti-vinculin [V9131; 1:20,000 western blotting (WB); 1:500 immunofluorescence (IF)] and anti-β tubulin (T4026; 1:2000) antibodies were purchased from Sigma (Saint Louis, MO). Mouse anti-β-actin (ab6276; 1:10,000) and rabbit anti-vinculin (ab73412; 1:100 IF) antibodies were purchased from Abcam (Cambridge, UK). Mouse anti- YAP (sc-101199; 1:100 IF, 1:1000 WB), rabbit anti-ERK2 (sc-154; 1:10,000) and goat anti-lamin B (sc-6216; 1:100) antibodies were purchased from Santa Cruz Biotechnology (Santa Cruz, CA). Rabbit anti-aP2 (#3544;1:2000), rabbit anti-phospho-YAP (#4911; 1:1,000), rabbit anti-LATS1 (#3477; 1:1000) and rabbit anti-phospho LATS1 (#9157; 1:1000) antibodies were purchased from Cell Signaling Technology (Boston, MA). Rabbit anti-vinexin polyclonal antibody was described previously (40). Alexa-Fluor-568 phalloidin was purchased from Thermo (Rockford, IL). Type I collagen was purchased from Nitta Gelatin (Osaka, Japan). Insulin, IBMX and cytochalasin D were purchased from Sigma-Aldrich.

Cell culture and differentiation

ST2, a mouse bone-marrow-derived mesenchymal stem cell line, and UE7T-13, a

human bone-marrow-derived mesenchymal stem cell line, were obtained from RIKEN BRC (Tsukuba, Japan) and JCRB Cell Bank (Osaka, Japan), respectively. ST2 cells were maintained in RPMI1640 (Sigma) supplemented with 10% fetal bovine serum (FBS; Sigma, or Biosera, Boussens, France) at 37°C under a humidified atmosphere containing 5% CO_2. For adipocyte differentiation, 7.5×10^4 (or 1.5×10^5 in some cases) cells were seeded into six-well plates. Adipocyte differentiation was induced by the addition of 0.5 mM IBMX, 10 μg/ml insulin and 10 μM DEX. After incubation for 2 days, the medium were changed to that containing 5 μg/ml insulin, and then to maintenance medium every 2 days thereafter. UE7T-13 cells were maintained in DMEM (Nacalai Tesque, Kyoto, Japan) supplemented with 10% FBS. For adipocyte differentiation, medium was changed to differentiation medium (0.5 mM IBMX, 10 μg/ml insulin and 1 μM DEX) every 2 days.

Establishment of vinculin-depleted cells and vinculin reexpressing cells

Vinculin-depleted cells and vinculin re-expressing cells were established using lentivirus as described previously (11), with slight modifications. Briefly, lentiviruses for knockdown were generated by transfecting pMD2.G, psPAX2 (Addgene, Cambridge, MA) and pLKO.1 vectors, and lentiviruses for expression were generated by transfecting pMD2G, pRSV-Rev, pMDLg/pRRE (Addgene) and pCDH vectors. pLKO.1 harboring vinculin small hairpin RNA (mouse 5′-CCCTGTACTTTCAGTTACTAT-3′, or human 5′-GCCTAACAGGGAA GAGGTATT-3′) was purchased from Openbiosystems (Waltham, MA). pCDH-EF1-IRES-hygro vector was purchased from System Biosciences (Mountain View, CA) and vinculin was subcloned into the vector in a similar manner to that previously described (Yamashita et al., 2014). ST2 cells were infected with lentiviruses, followed by incubating with medium containing 3 μg/ml puromycin or 100 μg/ml hygromycin B. UE7T-13 cells were infected with lentiviruses,

followed by incubating with medium containing 0.5 μg/ml puromycin. siRNA-mediated knockdown ST2 cells were transfected with 2 nM Stealth™ RNAi siRNAs against TAZ (siTAZ#1, 5′-GGAAGGUGAUGAAUCAGCCUCUUGG-3′; siTAZ#2, 5′-GGAGUCCUUCUUUAA GGAGCCCGAU-3′; Invitrogen, Carlsbad, CA) or control siRNA (StealthTM RNAi Negative Control Medium GC Duplex#3, Cat. No. 12935-113) using Lipofectamine RNAiMAX Reagent (Invitrogen) as previously described (41). UE7T-13 cells were transfected for 24 h with 20 nM Stealth RNAi™ siRNAs against human vinculin (siVinculin#1, VCL-HSS111259; siVinculin#2, VCLHSS187662; Invitrogen) using Lipofectamine RNAiMAX Reagent (Invitrogen).

Preparation of PAA gel substrates

PAA gel substrate was prepared as previously described with slight modification (11, 42). Briefly, 35 μl of the acrylamide mix reagents (final proportions were 5–8% acrylamide monomer, 0.03–0.3% bisacrylamide, 0.05% ammonium persulfate and 0.1% TEMED) was dropped onto glass coverslips or glassbottom dishes. The polyacrylamide gels were coated with 200 μg/ml type I collagen (Nitta Gelatin) using sulfo-SANPAH (ProteoChem, IL). The elastic moduli of the gels were from 1.5 kPa to 23 kPa.

Western blotting

Whole-cell lysates were prepared in lysis buffer (1% SDS and 1% protease inhibitor cocktail (Roche) in PBS). Amounts of lysates obtained from cells cultured on PAA gels were adjusted according to the DNA concentration. DNA concentration was measured using the Qubit dsDNA HS Assay Kit (Invitrogen). Protein concentrations of lysates obtained from cells on plastic dishes were determined with BCA reagents (Thermo) and equal amounts of lysates were analyzed by SDS-PAGE and western blotting using specific antibodies. Secondary antibodies

conjugated to horseradish peroxidase (HRP) were used, and bound antibodies were detected using Immunostar LD/Zeta (Wako, Osaka, Japan) and EZ-Capture (ATTO, Tokyo, Japan).

Oil red O staining

Cells were washed twice with PBS and fixed with 3.7% formaldehyde in PBS for 15 min at room temperature. After washing with 60% isopropanol in distilled water, the cells were stained with 0.18% (w/v) Oil Red O in 60% isopropanol for 30 min, followed by washing with 60% isopropanol once and PBS twice. Images of stained cells were obtained by microscopy (Nikon ECLIPSE TE300-2) equipped with a Leica MC120HD camera. For cells cultured on PAA gels, an additional wash with 40% isopropanol and 20% isopropanol was performed. Quantification of Oil Red O-stained area was performed using ImageJ software (National Institutes of Health, Bethesda, MD).

qRT-PCR

qRT-PCR was performed as described previously (43). Briefly, total RNA was extracted using an RNeasy mini kit (QIAGEN, Hilden, Germany), and cDNA was synthesized using Super Script reverse transcriptase III (Invitrogen). qRT-PCR analysis was carried out with Step One™ Real-Time PCR Systems (Applied Biosystems) using Fast SYBR® Green Master Mix (Applied Biosystems). Relative expression levels to internal control GAPDH (or 36B4, RPS18 in some cases) were given. Sequences of specific primers used in this paper are summarized in Table 1.

Immunostaining and quantification of FAs

Immunostaining was performed to analyze the total amount of vinculin or the amount of vinculin that was resistant to CSK buffer treatment as described previously (11), with slight

Table. 1 sequences of primers

Target		sequence	host
GAPDH	forward	5'-CATGGCCTTCCGTGTTCCTA-3'	mouse
	reverse	5'-GCGGCACGTCAGATCCA-3'	
36B4	forward	5'-TGTGTGTCTGCAGATCGGGTAC-3'	mouse
	reverse	5'-CTTTGGCGGGATTAGTCGAAG-3'	
PPARγ2	forward	5'-AACTCTGGGAGATTCTCCTGTTGA-3'	mouse
	reverse	5'-TGGTAATTTCTTGTGAAGTGCTCATA-3'	
aP2	forward	5'-GAAGACAGCTCCTCCTCGAAGGTT-3'	mouse
	reverse	5'-TGACCAAATCCCCATTTACGC-3'	
MyoD	forward	5'-GCCGGTGTGCATTCCAA-3'	mouse
	reverse	5'-CACTCCGGAACCCCAACAG-3'	
SOX9	forward	5'-ACCCACCACTCCCAAAACC-3'	mouse
	reverse	5'-CGCCCCTCTCGCTTCAG-3'	
Runx2	forward	5'-GCCGAGCTCCGAAATGC-3'	mouse
	reverse	5'-AGATCGTTGAACCTGGCTACTTG-3'	
ALP	forward	5'-ACCGCTGCCCGAATCC-3'	mouse
	reverse	5'-TCTCCTCGCCCGTGTTGT-3'	
Osteopontin	forward	5'-TCTGATGAGACCGTCACTGC-3'	mouse
	reverse	5'-TGTCCTTGTGGCTGTGAAAC-3'	
CTGF	forward	5'-AAAGTGCATCCGGACACCTAA-3'	mouse
	reverse	5'-TGCAGCCAGAAAGCTCAAACT-3'	
Ankrd1	forward	5'-CTCAGCACAGCGCTGCAT-3'	mouse
	reverse	5'-TGCTCAGCGCACTCGTAATG-3'	
GAPDH	forward	5'-GGCATCCTGGGCTACACTGA-3'	human
	reverse	5'-GGAGTGGGTGTCGCTGTTG-3'	
PPARg2	forward	5'-GCTGTTATGGGTGAAACTCTG-3'	human
	reverse	5'-ATAAGGTGGAGATGCAGGTTC-3'	
aP2	forward	5'-TGGTTGATTTTCCATCCCAT-3'	human
	reverse	5'-TACTGGGCCAGGAATTTGAC-3'	
CTGF	forward	5'-TGCACCGCCAAAGATGGT-3'	human
	reverse	5'-GACTCTCCGCTGCGGTACAC-3'	
Ankrd1	forward	5'-GACCTCAACGCCAAAGACAGA-3'	human
	reverse	5'-GGTTCAGTCTCACCGCATCA-3'	

modifications. Briefly, to analyze total vinculin, cells cultured on PAA gel substrates were fixed with 1.5% paraformaldehyde at 4°C for 45 min, followed by permeabilization with PBS containing 0.2% Triton X-100 for 5 min at room temperature. To analyze CSK-resistant vinculin, cells were first treated twice with CSK buffer (0.1% Triton X-100, 10 mM PIPES, pH 6.8, 50 mM NaCl, 3 mM $MgCl_2$, 300 mM sucrose) at 4°C for 30 s, followed by fixation with 4% paraformaldehyde for 15 min at room temperature. Cells were treated with 10% goat serum (or donkey serum in some cases) in PBS for blocking, and were incubated with primary antibodies at 4°C overnight and with secondary antibodies for 1 h. Images were obtained with a LSM700 confocal microscope (Carl Zeiss, Oberkochen, Germany) with a ×40 oil immersion Plan-APOCHROM objective lens, or with a Nikon C2 confocal microscope (Nikon, Tokyo, Japan) with a ×40 Plan-APO objective lens. Quantification of the total number and average area of vinculin at FAs per cell was performed using ImageJ software as described previously (11).

Quantification of YAP/TAZ nuclear localization

Cells were seeded on PAA gels or collagen-coated glass coverslips at a density of 7.5×10^4 or 1.5×10^5 cells per well. At 24 h after seeding, cells were fixed with 4% paraformaldehyde for 15 min, followed by permeabilization with PBS containing 0.2% Triton X-100 for 5 min. Immunostaining was performed as described above. YAP/TAZ nuclear localization was evaluated by assessing the nucleus-to-cytosol intensity ratio. Intensity inside the nucleus and just outside the nucleus was quantified using ImageJ.

Statistical analysis

Statistical analysis was performed in Origin 8.5.1 software. Values that displayed a normal distribution were analyzed with a Tukey's honest significant difference test after one-way

ANOVA or Student's t-test for comparison among three or more groups or between two groups, respectively. Values that did not display a normal distribution were analyzed with a Mann–Whitney U-test after Kruskal–Wallis's ANOVA for comparison among three or more groups.

REFERENCES

1. Varelas X (2014) The Hippo pathway effectors TAZ and YAP in development, homeostasis and disease. *Development* 141(8):1614-1626.
2. Seo E, *et al.* (2013) SOX2 regulates YAP1 to maintain stemness and determine cell fate in the osteo-adipo lineage. *Cell Rep* 3(6):2075-2087.
3. Hong JH, *et al.* (2005) TAZ, a transcriptional modulator of mesenchymal stem cell differentiation. *Science* 309(5737):1074-1078.
4. Aragona M, *et al.* (2013) A mechanical checkpoint controls multicellular growth through YAP/TAZ regulation by actin-processing factors. *Cell* 154(5):1047-1059.
5. Cui Y, *et al.* (2015) Cyclic stretching of soft substrates induces spreading and growth. *Nat Commun* 6:6333.
6. Dupont S, *et al.* (2011) Role of YAP/TAZ in mechanotransduction. *Nature* 474(7350):179-183.
7. Wada K, Itoga K, Okano T, Yonemura S, & Sasaki H (2011) Hippo pathway regulation by cell morphology and stress fibers. *Development* 138(18):3907-3914.
8. Hwang JH, *et al.* (2015) Extracellular Matrix Stiffness Regulates Osteogenic Differentiation through MAPK Activation. *PLoS One* 10(8):e0135519.
9. Swift J, *et al.* (2013) Nuclear lamin-A scales with tissue stiffness and enhances matrix-directed differentiation. *Science* 341(6149):1240104.
10. Holle AW, *et al.* (2013) In situ mechanotransduction via vinculin regulates stem cell differentiation. *Stem Cells* 31(11):2467-2477.
11. Yamashita H, *et al.* (2014) The role of the interaction of the vinculin proline-rich linker region with vinexin α in sensing the stiffness of the extracellular matrix. *J Cell Sci* 127(Pt 9):1875-1886.
12. Kanai F, *et al.* (2000) TAZ: a novel transcriptional co-activator regulated by interactions with 14-3-3 and PDZ domain proteins. *EMBO J* 19(24):6778-6791.
13. Bourdet-Sicard R, *et al.* (1999) Binding of the Shigella protein IpaA to vinculin induces F-actin depolymerization. *EMBO J* 18(21):5853-5862.
14. Wen KK, Rubenstein PA, & DeMali KA (2009) Vinculin nucleates actin polymerization and modifies actin filament structure. *J Biol Chem* 284(44):30463-30473.

15. Thompson PM, *et al.* (2014) Identification of an actin binding surface on vinculin that mediates mechanical cell and focal adhesion properties. *Structure* 22(5):697-706.
16. Cohen DM, Chen H, Johnson RP, Choudhury B, & Craig SW (2005) Two distinct head-tail interfaces cooperate to suppress activation of vinculin by talin. *J Biol Chem* 280(17):17109-17117.
17. Mori T, *et al.* (2005) Combination of hTERT and bmi-1, E6, or E7 induces prolongation of the life span of bone marrow stromal cells from an elderly donor without affecting their neurogenic potential. *Mol Cell Biol* 25(12):5183-5195.
18. Engler AJ, Sen S, Sweeney HL, & Discher DE (2006) Matrix elasticity directs stem cell lineage specification. *Cell* 126(4):677-689.
19. Lee JS, Ha L, Kwon IK, & Lim JY (2013) The role of focal adhesion kinase in BMP4 induction of mesenchymal stem cell adipogenesis. *Biochem Biophys Res Commun* 435(4):696-701.
20. Thompson WR, *et al.* (2013) Mechanically activated Fyn utilizes mTORC2 to regulate RhoA and adipogenesis in mesenchymal stem cells. *Stem Cells* 31(11):2528-2537.
21. Uzer G, *et al.* (2015) Cell Mechanosensitivity to Extremely Low-Magnitude Signals Is Enabled by a LINCed Nucleus. *Stem Cells* 33(6):2063-2076.
22. Dong J, *et al.* (2007) Elucidation of a universal size-control mechanism in Drosophila and mammals. *Cell* 130(6):1120-1133.
23. Zhao B, *et al.* (2007) Inactivation of YAP oncoprotein by the Hippo pathway is involved in cell contact inhibition and tissue growth control. *Genes Dev* 21(21):2747-2761.
24. Jockusch BM & Isenberg G (1981) Interaction of alpha-actinin and vinculin with actin: opposite effects on filament network formation. *Proc Natl Acad Sci U S A* 78(5):3005-3009.
25. Menkel AR, *et al.* (1994) Characterization of an F-actin-binding domain in the cytoskeletal protein vinculin. *J Cell Biol* 126(5):1231-1240.
26. Le Clainche C, Dwivedi SP, Didry D, & Carlier MF (2010) Vinculin is a dually regulated actin filament barbed end-capping and side-binding protein. *J Biol Chem* 285(30):23420-23432.
27. Holle AW, *et al.* (2016) High content image analysis of focal adhesion-dependent mechanosensitive stem cell differentiation. *Integr Biol (Camb)* 8(10):1049-1058.
28. Janoštiak R, *et al.* (2014) CAS directly interacts with vinculin to control mechanosensing and focal adhesion dynamics. *Cell Mol Life Sci* 71(4):727-744.
29. Grashoff C, *et al.* (2010) Measuring mechanical tension across vinculin reveals regulation of focal adhesion dynamics. *Nature* 466(7303):263-266.
30. Hirata H, Tatsumi H, Lim CT, & Sokabe M (2014) Force-dependent vinculin binding to

talin in live cells: a crucial step in anchoring the actin cytoskeleton to focal adhesions. *Am J Physiol Cell Physiol* 306(6):C607-620.

31. Koshimizu T, *et al.* (2012) Vinculin functions as regulator of chondrogenesis. *J Biol Chem* 287(19):15760-15775.
32. Overholtzer M, *et al.* (2006) Transforming properties of YAP, a candidate oncogene on the chromosome 11q22 amplicon. *Proc Natl Acad Sci U S A* 103(33):12405-12410.
33. Sorrentino G, *et al.* (2014) Metabolic control of YAP and TAZ by the mevalonate pathway. *Nat Cell Biol* 16(4):357-366.
34. Wang W, *et al.* (2015) AMPK modulates Hippo pathway activity to regulate energy homeostasis. *Nat Cell Biol* 17(4):490-499.
35. Calvo F, *et al.* (2013) Mechanotransduction and YAP-dependent matrix remodelling is required for the generation and maintenance of cancer-associated fibroblasts. *Nat Cell Biol* 15(6):637-646.
36. Rubashkin MG, *et al.* (2014) Force engages vinculin and promotes tumor progression by enhancing PI3K activation of phosphatidylinositol (3,4,5)-triphosphate. *Cancer Res* 74(17):4597-4611.
37. Ruiz C, *et al.* (2011) Amplification and overexpression of vinculin are associated with increased tumour cell proliferation and progression in advanced prostate cancer. *J Pathol* 223(4):543-552.
38. Wang Y, *et al.* (2012) Proteomic differential display identifies upregulated vinculin as a possible biomarker of pancreatic cancer. *Oncol Rep* 28(5):1845-1850.
39. Elosegui-Artola A, *et al.* (2016) Mechanical regulation of a molecular clutch defines force transmission and transduction in response to matrix rigidity. *Nat Cell Biol* 18(5):540-548.
40. Kioka N, *et al.* (1999) Vinexin: a novel vinculin-binding protein with multiple SH3 domains enhances actin cytoskeletal organization. *J Cell Biol* 144(1):59-69.
41. Tomiyama L, Sezaki T, Matsuo M, Ueda K, & Kioka N (2015) Loss of Dlg5 expression promotes the migration and invasion of prostate cancer cells via Girdin phosphorylation. *Oncogene* 34(9):1141-1149.
42. Damljanović V, Lagerholm BC, & Jacobson K (2005) Bulk and micropatterned conjugation of extracellular matrix proteins to characterized polyacrylamide substrates for cell mechanotransduction assays. *Biotechniques* 39(6):847-851.
43. Sezaki T, *et al.* (2012) Role of Dlg5/lp-dlg, a membrane-associated guanylate kinase family protein, in epithelial-mesenchymal transition in LLc-PK1 renal epithelial cells. *PLoS One* 7(4):e35519.

CHAPTER 2

Roles of SORBS family proteins in the differentiation of mesenchymal stem cells

CHAPTER 2

Roles of SORBS family proteins in the differentiation of mesenchymal stem cells

It has been previously revealed that the ECM stiffness-dependent regulation of vinculin requires its binding to other FA protein SORBS1 (also known as c-Cbl Associated Protein (CAP)/ponsin) or SORBS3 (also known as vinexin α) (1). Vinexin is required for ECM stiffness-dependent migration in mouse embryonic fibroblasts (2). SORBS family in mammal consists of vinexin, CAP and Arg-binding protein 2 (also known as SORBS2) (ArgBP2) (3, 4). These proteins share the same domain structures, containing a sorbin homology (SoHo) domain and three Src homology 3 (SH3) domains (Fig. 1A). Despite the fact that SORBS family proteins have functional redundancy, including binding partners and ECM stiffness-dependent regulation of vinculin, downstream signals and phenotype of knockout (KO) mice differ from each other: Vinexin KO mice shows an increase in cardiac hypertrophy and delay in wound healing (4, 5). CAP is involved in PI3K-independent insulin signaling (6, 7) and CAP KO mice show improved insulin resistant under high-fat diet (8). ArgBP2 are involved in regulation of intracellular tension (1, 9) and ArgBP2 KO mice show reduced long-term memory (10). However, whether SORBS proteins regulate differentiation of MSCs in an ECM stiffness-dependent manner remains still unclear.

In this study, the author shows that vinexin and CAP function as mechanosensors to regulate ECM stiffness-dependent nuclear localization of YAP/TAZ in MSC. In addition, vinexin and CAP are involved in MSC differentiation into adipocytes in a manner dependent on ECM stiffness.

RESULTS

Vinexin and CAP contributes to cytoskeletal association of vinculin in mesenchymal stem cells

The author first checked the expression of vinexin family proteins in ST2, a mouse mesenchymal stem cell line (Fig. 1B). Expression of both vinexin α and β (transcriptional variants) as well as CAP were detected by western blotting, while expression of ArgBP2 was not detected (data not shown). To investigate roles of vinexin and CAP in the differentiation of mesenchymal stem cells, vinexin and CAP were stably knocked down using shRNA lentivirus. Expression of vinexin α, which has been reported to function as a sensor for ECM stiffness (2), was reduced to less than 1% in two vinexin-depleted cell lines (Fig. 1B). CAP is known to have several splice variants (11). The most prominent signal was detected at approximately 130 kDa in ST2 cells (Fig. 1B). Expressions of CAP variants were reduced to 6.4%(#1) and 13%(#2), respectively, in CAP-depleted cells (Fig. 1B). Immunostaining analysis showed that the amounts of vinexin and CAP localized both in cytosol and FAs were decreased (Fig. 1C,D).

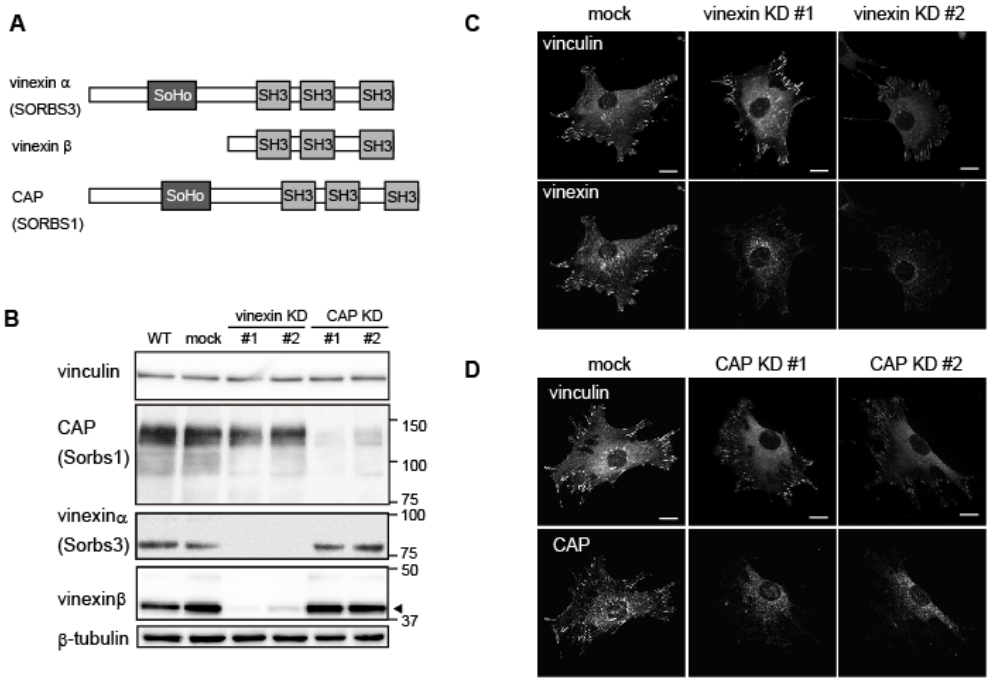

Fig. 1. Expression of vinexin and CAP in ST2 cells. (A) Schematic diagram of the domain structure of SORBS proteins (vinexin α and β, CAP). (B) Cell lysates were analyzed using western blotting. β-tubulin was checked as loading control. (C,D) Localization of vinculin, vinexin, and CAP were analyzed with immunostaining. Scal bars: 20 μm.

Vinexin α and CAP contribute to CSK (cytoskeleton stabilization buffer)-resistance of vinculin, which represents the fraction of vinculin tightly bound to the cytoskeleton (that is, open form of vinculin), in mouse embryonic fibroblasts on rigid substrates (1). Thus, the author first asked whether vinexin or CAP is required for localization at FAs and cytoskeletal association of vinculin on rigid (glass) substrates in ST2 cells. The vinculin localization was examined using normal immunostaining (Fig. 2A). Quantified data showed that numbers and total area of FAs per cell in vinexin- and CAP-depleted cells were comparable with control cells, indicating that vinexin and CAP are dispensable for vinculin localization at FAs in ST2 cells (Fig. 2B). On the other hand, FAs containing CSK-resistant vinculin were significantly decreased in vinexin- or CAP-depleted cells (Fig. 2C,D). These results demonstrate that vinexin and CAP are necessary for cytoskeletal association of vinculin in mesenchymal stem cells on rigid substrates.

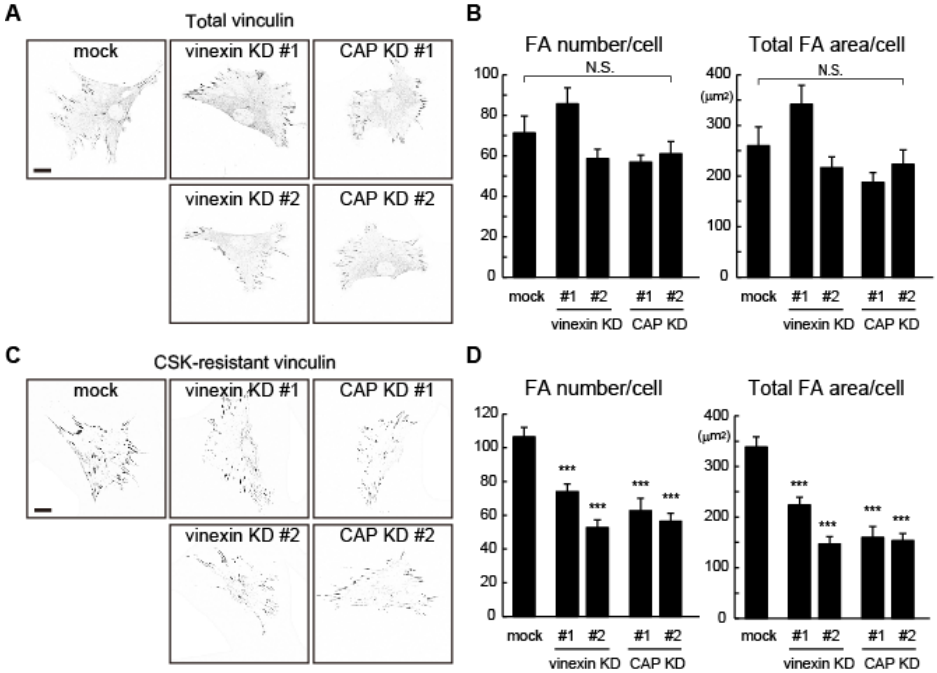

Fig. 2 Vinexin and CAP were required for the cytoskeletal association of vinculin in mesenchymal stem cells. (A–D) Control (mock), vinexin-depleted cells (vinexin KD), and CAP-depleted cells (CAP KD) on glass substrates coated with 10 μg/ml type-I collagen I (1.0×10^4 cells/ 12 well plates) were fixed without (A,B) or with (C,D) CSK treatment. Cells were immunostained using anti-vinculin antibody. Images were obtained using confocal microscopy, and the gray images were inverted to increase their visibility (A,C). The number of FAs and total FA area in each cell were quantified using ImageJ (B,D). Fifteen cells from two separate experiments were analyzed. The values represent the mean±s.e.m. Statistical significance was determined by one-way ANOVA with Tukey's test (B,D). ***: $p<0.001$. Scale bars: 20 μm.

Vinexin and CAP promote the nuclear localization of YAP/TAZ on rigid ECM

Vinculin promotes nuclear localization of transcriptional factor YAP/TAZ in an ECM stiffness-dependent manner, whereas vinculin mutated in proline-rich linker region, where both vinexin and CAP bind (12), has less effect (13). Therefore, the author investigated the effects of vinexin and CAP on the nuclear localization of YAP/TAZ. Vinexin- and CAP-depleted cells were seeded onto rigid (glass) substrates and immunostained using anti-YAP/TAZ antibody (Fig. 3A). Both vinexin and CAP depletion decreased the YAP/TAZ nuclear localization. Quantitative analysis indicated that the YAP/TAZ intensity ratio of nucleus to cytosol were decreased in the

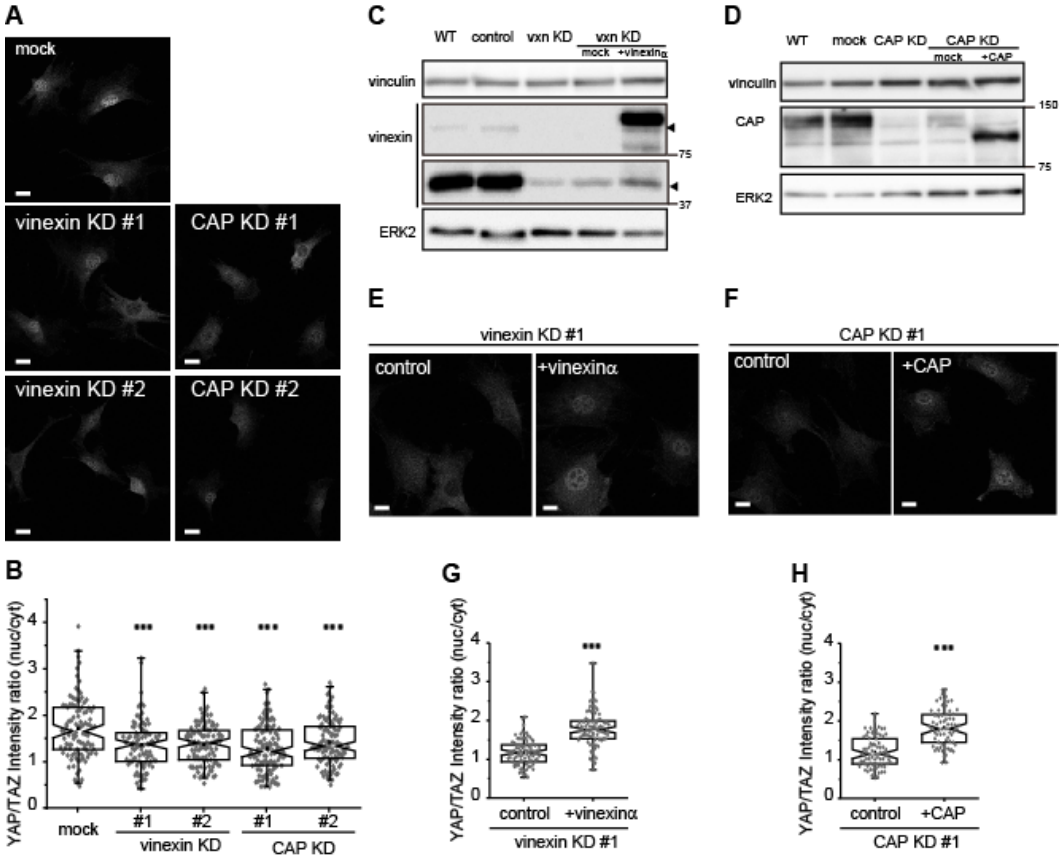

Fig. 3 Vinexin and CAP promoted the nuclear localization of YAP/TAZ. (A,B) Cells were seeded on glass substrates coated with 10 μg/ml collagen I with the density of 2.0×10^4 cells/ 12 well plates and fixed 24 hours after seeding. Cells were immunostained with anti-YAP/TAZ antibody and nucleus were visualized with Hoechst 33342. (B,G,H) The intensity ratio (nuc/cyt) of YAP/TAZ was quantified. At least 70 cells were analyzed from two separate experiment. (C,D) Vinexin- or CAP-reexpressing cells were established and these expressions were analyzed by western blotting. (E-H) Control, and vinexin α- or CAP- re-expressing cells in KD cells were seeded on glass substrates and immunostained with anti YAP-TAZ antibody. Each experiments were performed twice. Statistical significance was determined by Kruskal–Wallis's ANOVA with Mann–Whitney's U-test (B,E,F). ***: $p<0.001$.

vinexin- or CAP-depleted cells compared to that in control cells (Fig. 3B). No significant differences were observed in the intensity ratio between vinexin- and CAP-depleted cells. To confirm these data, vinexin-depleted cells re-expressing vinexin α (referred to vinexin α re-expressing cells) and CAP-depleted cells re-expressing CAP (referred to CAP re-expressing cells) were established (Fig. 3C,D). Re-expression of vinexin α and CAP rescued the decrease in the nuclear localization of YAP/TAZ (Fig. 3E-H). These results indicate that vinexin and CAP promote the nuclear localization of YAP/TAZ on rigid substrates.

To explore the effect of vinexin and CAP depletion on ECM stiffness-regulated YAP/TAZ nuclear localization, vinexin- and CAP-depleted cells were seeded onto polyacrylamide (PAA) gels with different levels of stiffness in the range from 1.5 kPa to 42 kPa (Fig. 4). Consistent with the results in Chapter 1, moderate rigidity (8.7 kPa) increased the intensity ratio to 1.72 ± 0.05 compared to 1.13 ± 0.04 on soft substrates (1.5 kPa) in control cells (Fig. 4B). Stiffer substrates (23 kPa and 42 kPa) further increased the intensity ratio to 1.95 ± 0.05 and 2.31 ± 0.05, respectively. In contrast, the increase in the intensity ratio in vinexin- and CAP-depleted cells on substrates with 8.7 kPa of stiffness were only moderately, to 1.39 ± 0.04 and

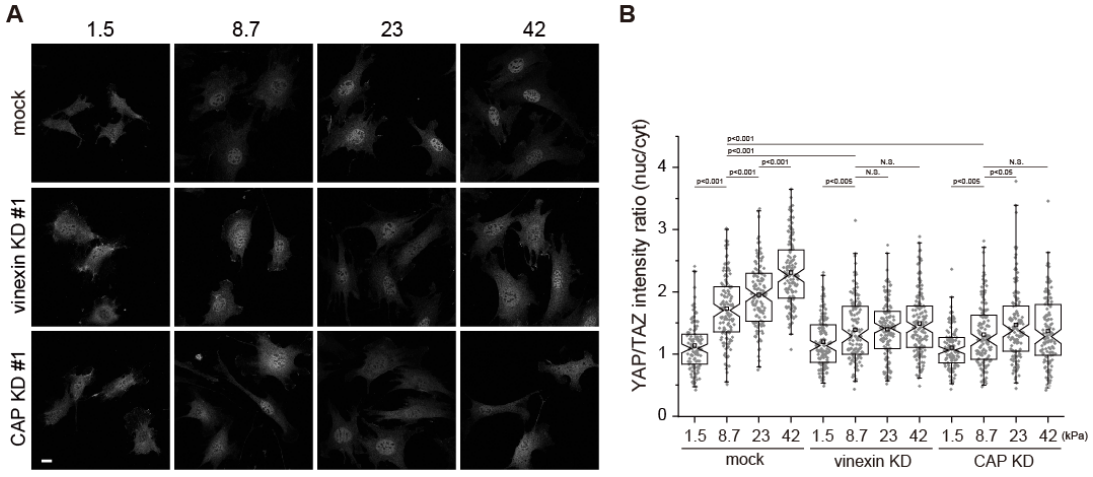

Fig. 4 Vinexin and CAP promoted the nuclear localization of YAP/TAZ in a ECM stiffness-dependent manner. (A,B) Control cells and vinexin- or CAP- depleted cells (6.0×10^4 cells/ 35 mm dish) on collagen coated PAA gels with different levels of stiffness (1.5 kPa, 8.7 kPa, 23 kPa, 42 kPa) were immunostained with anti-YAP/TAZ antibody. (B) The quantified intensity ratio from at least 100 cells were shown. The experiment was repeated twice. Statistical significance was determined by Kruskal–Wallis's ANOVA with Mann–Whitney's U-test. Scale bars: 20 μm.

1.30 ± 0.04, respectively. Furthermore, no significant increase were observed on gels above 8.7 kPa in vinexin-depleted cells. A similar tendency was observed in CAP-depleted cells. Taken together, both vinexin and CAP are required for the promotion of the YAP/TAZ nuclear localization on rigid substrates.

CAP inhibits the adipocyte differentiation, whereas vinexin has the opposite effect

As shown in Chapter 1, vinculin inhibits the adipocyte differentiation, whereas promotes the osteoblast differentiation on rigid substrates via promoting nuclear localization of YAP/TAZ. Thus, the author investigated a role of vinexin and CAP in the regulation of MSC differentiation. The author first checked the temporal expression pattern of vinexin and CAP in wild-type (WT) ST2 cells during differentiation into adipocytes or osteoblasts by western blotting (Fig. 5). Expression of vinexin α was increased, possibly due to the cell density, prior to induction of differentiation (day 0). The expression of vinexin α were maintained during the progression of adipocyte differentiation, while decreased accompanying the progression of osteoblast differentiation. Vinexin β remained constant throughout the differentiation both into adipocytes and osteoblasts. In contrast, the expression of CAP was decreased prior to induction of differentiation (day 0), then upregulated during adipogenesis and osteogenesis. These results suggest a role of SORBS proteins during differentiation of mesenchymal stem cells.

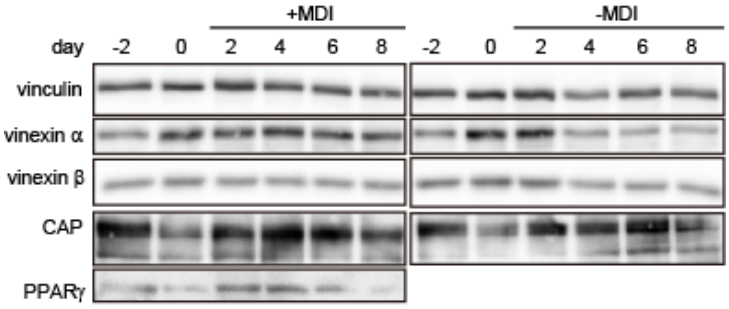

Fig.5 Temporal expressions of vinexin and CAP during differentiation
Equal amounts of cell lysates were analyzed by western blotting using the anti-vinculin, anti-vinexin, anti-CAP, anti-PPARγ antibodies.

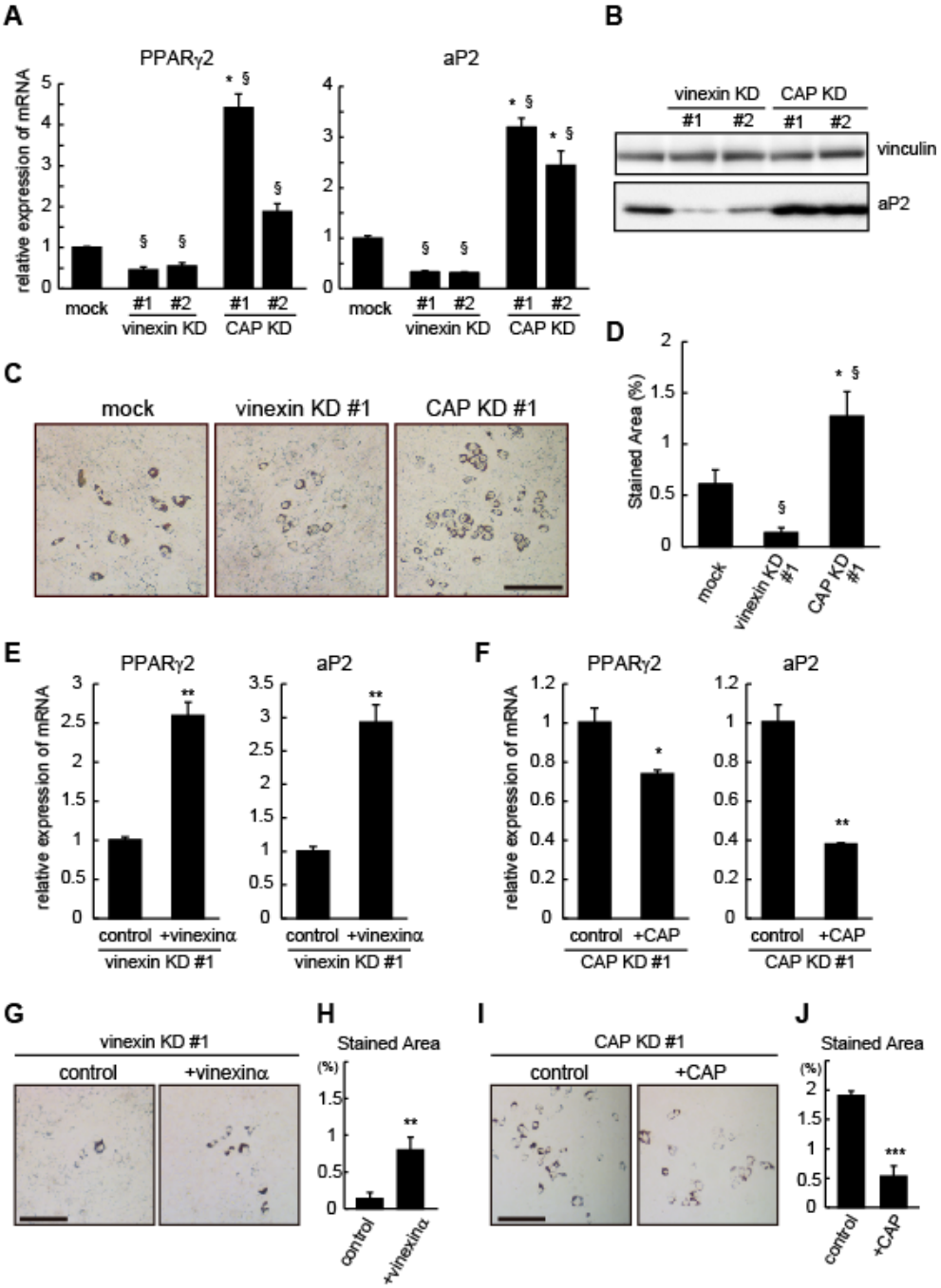

Fig. 6 CAP suppressed but vinexin promoted adipocyte differentiation adipogenesis on rigid substrates. Vinexin- or CAP-depleted (A-D) cells, vinexin α re-expressing cells (E,G,H) or CAP re-expressing cells (F,I,J) were seeded on plastic dishes, and induced to differentiate into adipocyte. RNAs were extracted 6 day after MDI treatment and the expression of mRNAs encoding PPARg2 and aP2 was quantified by qRT-PCR (A,E-F). The relative expression compared to control cells are shown. (B) Cell were lysed and equate amounts of cell lysates were analyzed by western blotting using the anti-aP2 and anti-vinculin (loading control) antibodies. (C-D,G-J) Cells were stained with Oil Red O on day 6 after MDI treatment and representative images are shown (C,G,I). Scale bars: 200 μm. (D) Nine images were obtained from three independent experiments, and the percentage of area stained was quantified with ImageJ. The values represent the mean±s.e.m. Statistical significance was determined by one-way ANOVA with Tukey's test or Student's t-test (E,F,H,J). ***: $p<0.001$ (by Tukey's test). §: $p<0.001$ (compared to mock by Student's t-test).

To examine the role of vinexin and CAP in the differentiation of mesenchymal stem cells, the author tested the differentiation of vinexin- and CAP-depleted cells into adipocyte on rigid (plastic) substrates. qRT-PCR analysis showed that depletion of CAP increased the expression of adipogenic markers, PPARγ2 (4.4 ± 0.01-fold (#1) and 1.9 ± 0.01-fold (#2)) and aP2 (3.2 ± 0.06-fold (#1) and 2.4 ± 0.12-fold (#2) (Fig. 6A). On the other hand, unexpectedly, the depletion of vinexin decreased the expression of these adipogenic markers, PPARγ2 (0.5 ± 0.17-fold (#1) and 0.6 ± 0.14-fold (#2)) and aP2 (0.3 ± 0.10-fold (#1) and 0.3 ± 0.04-fold (#2)). Western blotting analysis also showed that CAP depletion increased expression of aP2 protein while vinexin depletion decreased (Fig. 6B). Furthermore, Oil Red O staining analysis showed that lipid accumulation was increased by CAP-depletion but decreased by vinexin-depletion (Fig. 6C,D). Re-expression of vinexin α or CAP rescued the effects of depletion, as revealed by qRT-PCR analysis (Fig. 6E,F) and Oil Red O staining (Fig. 6G-J). Similar results obtained from vinexin-depleted murine C3H 10T1/2 cells (data not shown) support the role of vinexin in promotion of adipogenesis. Collectively, these results demonstrate that CAP inhibits the differentiation into adipocytes on rigid substrates, while vinexin promotes it.

CAP promotes but vinexin suppresses the differentiation into osteoblasts

The author next investigated the effect of vinexin and CAP depletion on osteoblast differentiation. Vinexin- or CAP-depleted cells were seeded onto rigid (plastic) substrates and induced to differentiate into osteoblasts. The mRNA expression of alkaline phosphatase (ALP), a marker for osteoblast differentiation, were down-regulated in CAP-depleted cells, whereas upregulated in vinexin depleted cells (Fig. 7A). Osteoblastic phenotype was further analyzed with ALP-activity staining (Fig. 7B,C). Quantified data showed that CAP depletion significantly decreased the ALP-activity staining compared to control cells (Fig. 7C). On the other hand,

vinexin depletion did not affect the staining. Re-expression of CAP rescued the decrease in ALP mRNA expression and activity staining (Fig. 7E,G,I). Re-expression of vinexin α rescued the mRNA expression, but again it did not affect ALP activity (Fig. 7D,F,H). Next, Alizarin Red S staining was performed to examine the effect on calcification. Vinexin-depletion increased the staining compare to control cells (Fig. 7J,K). CAP depletion slightly decreased it. It is possible

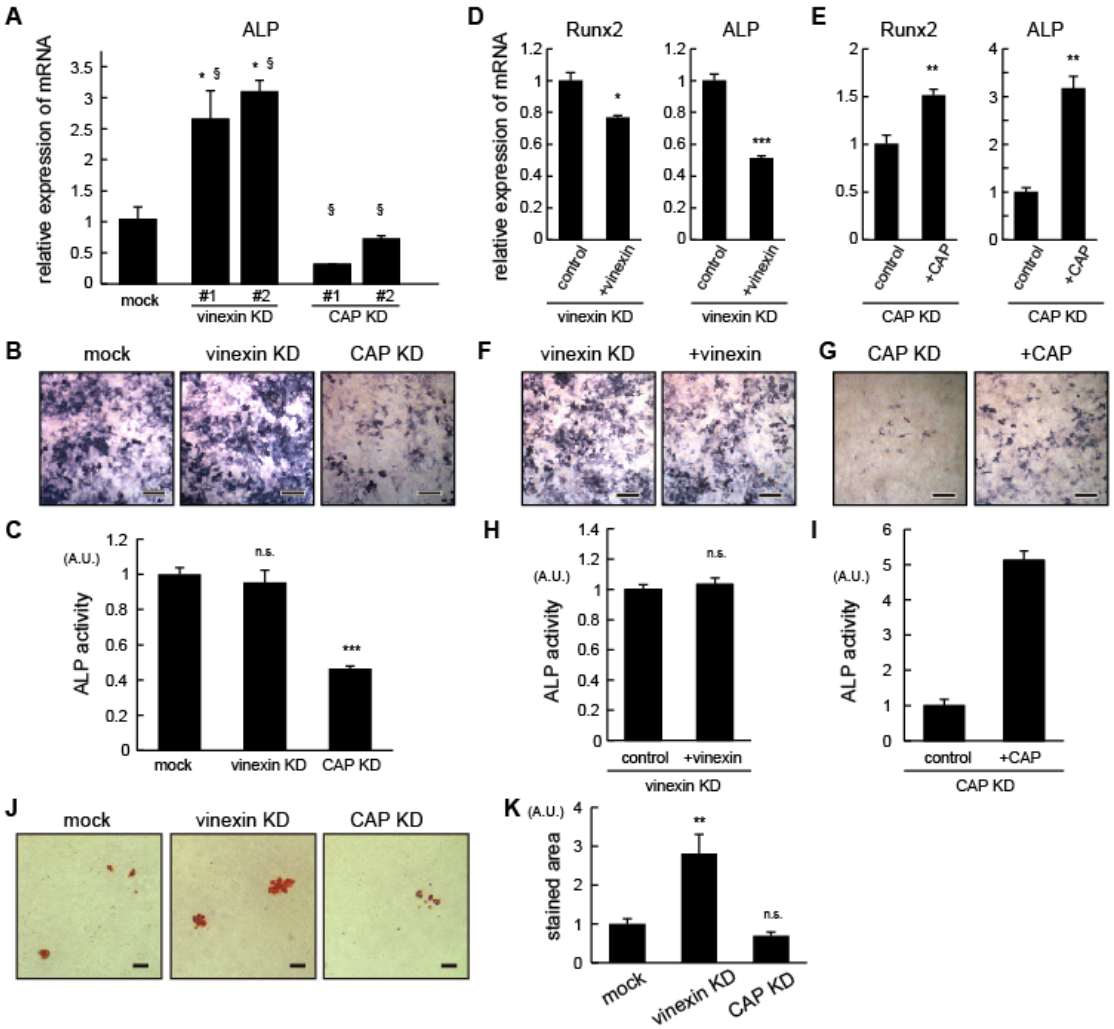

Fig. 7. CAP promoted osteoblast differentiation and vinexin inhibits calcification Vinexin- or CAP-depleted (A,B,C,J,K) cells and vinexin α re-expressing cells (D,F,H) or CAP re-expressing cells seeded on plastic dishes were induced to differentiate into osteoblasts by incubating with αMEM medium. (A,D,E) On day 6, RNAs were extracted and the expression of ALP mRNA was quantified by qRT-PCR. (B-C,F-I) On day 4, ALP activity were visualized and six images were obtained from two independent experiments for each condition. Scale bars: 400 μm. (C,H,I) Total intensity were quantified by ImageJ. (J,K) On day 6, cells were stained with Alizarin Red S and six images were obtained from two independent experiments. Scale bars: 200 μm. (K) The relative stained area was quantified with ImageJ. The values represent the mean±s.e.m. Statistical significance was determined by one-way ANOVA with Tukey's test (A,C,K) and Student's t-test (D,E,H,I). ***: $p<0.001$ (by Tukey's test). §: $p<0.01$ (compared to mock by Student's t-test).

that vinexin is involved in specific steps of the differentiation into osteoblasts. These results suggest that CAP promotes but vinexin suppresses the osteoblast differentiation.

CAP regulates the ECM stiffness-dependent differentiation into adipocytes

As shown in Chapter 1, vinculin attenuates the stiffness dependency of adipocyte differentiation in a stiffness range of 1.5 kPa to 8.7 kPa. In order to test the effects of vinexin and CAP on ECM stiffness-dependent differentiation, vinexin- or CAP-depleted cells were cultured on PAA gels with a stiffness range of 1.5 kPa to 23 kPa. Consistent to previous results, mock cells showed obvious stiffness-dependency of lipid droplet accumulation; rigid ECM (8.7 kPa and 23 kPa) significantly decreased the stained area to 43.8 ± 7.9% and 33.1 ± 6.0%, respectively, compared to soft ECM (1.5 kPa) (Fig. 8A,B). On the other hand, CAP depletion attenuated the ECM stiffness-dependent decrease in lipid droplet accumulation; rigid ECM decreased the stained area to 76.9 ± 11.0% (8.7 kPa) and 58.1 ± 6.8% (23 kPa) in CAP-depleted cells. Interestingly, there was no significant difference between control and CAP-depleted cells on soft ECM (1.5

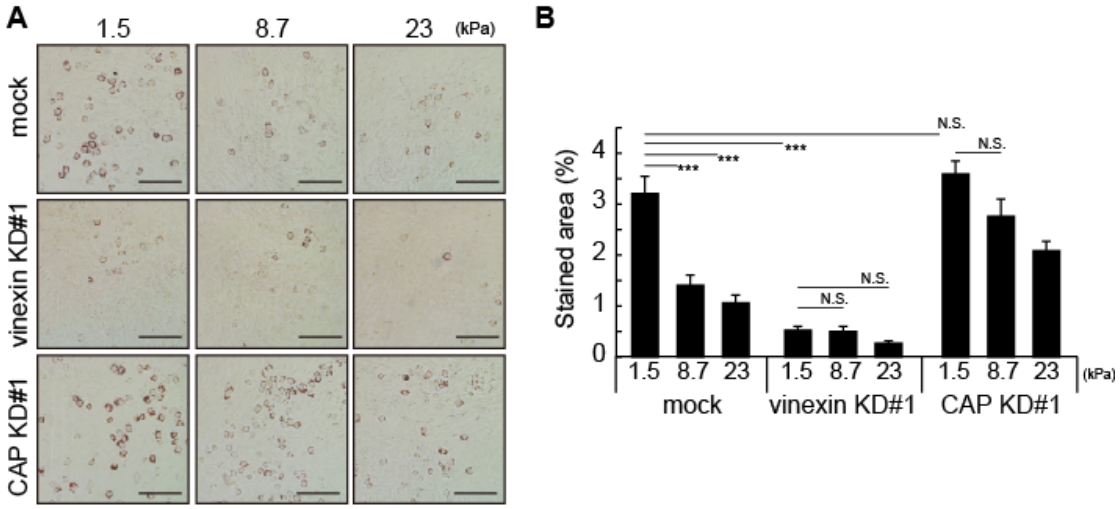

Fig. 8 Vinexin and CAP regulate the differentiation in a ECM stiffness-dependent manner. (A,B) Vinexin- or CAP-depleted cells were seeded onto PAA gels coated with collagen and induced to differentiate into adipocyte. Cells were stained with Oil Red O on day 6 after MDI treatment and representative images are shown. Scale bars: 200 μm. (B) Eight images were obtained from two independent experiments, and the percentage of area was quantified with ImageJ. Statistical significance was determined by one-way ANOVA with Tukey's test. ***: $p<0.001$.

kPa). In addition, vinexin depletion suppressed the accumulation of lipid droplets similar to that on rigid (plastic) substrates, and abolished that of ECM stiffness dependency. These observations suggest that vinexin and CAP contribute to the stiffness dependency of differentiation into adipocytes.

TAZ mediates the effect of CAP on the cell differentiation

In Chapter 1, the author demonstrated that vinculin inhibits adipogenesis via TAZ. To check whether CAP suppresses adipocyte differentiation via YAP/TAZ, TAZ was depleted by siRNAs in control or CAP-depleted cells and adipogenesis and osteogenesis were evaluated. Loss of TAZ expression was confirmed by western blotting (Fig. 9A). TAZ-knockdown increased the expression of aP2 by 20.9 ± 7.6% and decreased the expression of ALP by 50.4 ± 1.2% in control cells, whereas TAZ-knockdown hardly affected these expressions in CAP depleted cells (Fig. 9B).

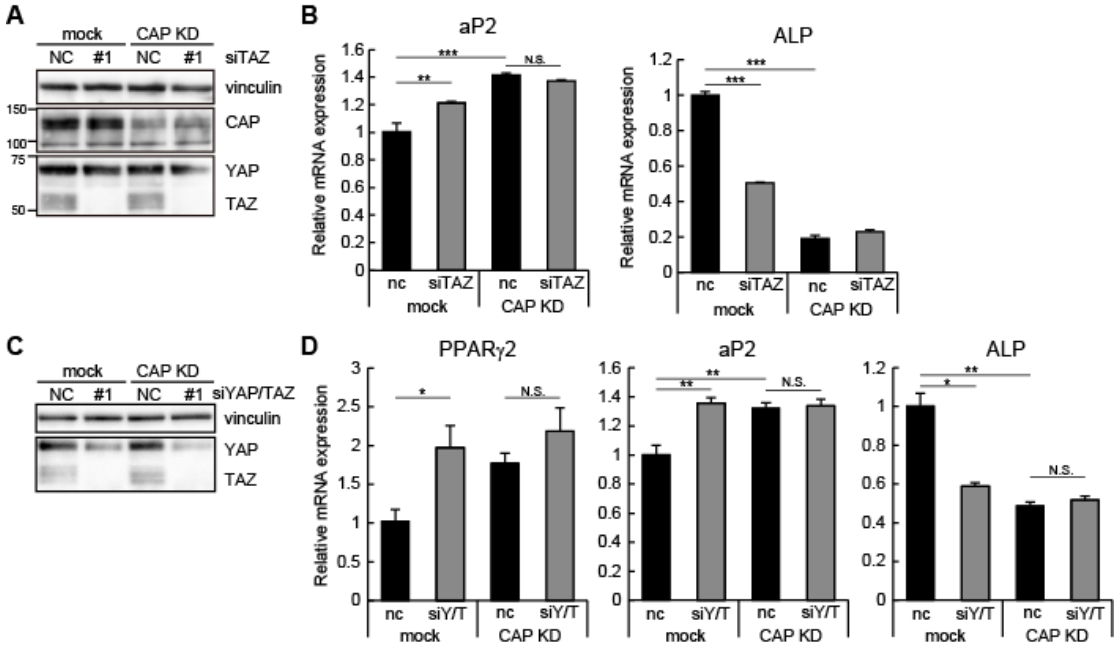

Fig. 9 Effect of YAP/TAZ knockdown on adipocyte differentiation of vinculin. CAP-depleted cells were transfected with negative control (siNC), TAZ-targeted siRNA (A,B) or the mixture of YAP siRNA and TAZ siRNA(C,D). (A,C) YAP and TAZ expression was analyzed with western blotting. (B,D) On day 6 after siRNA transfection, the expression of aP2 and ALP mRNA were quantified by qRT-PCR. The relative expression to that with negative control siRNA in control cells is shown from triplicate experiments. The values represent the mean±s.e.m. Each experiments were repeated twice. Statistical significance was determined by one-way ANOVA with Tukey's test. *: $p<0.05$. **: $p<0.01$. ***: $p<0.001$.

To further analyze this effect, YAP and TAZ were simultaneously depleted by the mixture of siRNAs targeted for YAP and TAZ. Similar effects were observed in YAP/TAZ knockdown cells (Fig. 9C,D). Taken together, these results indicate that CAP inhibits adipocyte differentiation through promoting TAZ nuclear localization.

DISCUSSION

Advances in materials of substrates with different levels of stiffness enabled us to reveal the underlying mechanism by which ECM stiffness regulates the differentiation of stem cell via adhesion molecules (14, 15). SORBS family proteins, vinexin α and CAP, are required for stabilizing actin high-affinity form of vinculin in fibroblasts (1). However, it has been still unclear whether SORBS family proteins regulate mechano-signal transduction and regulate differentiation of mesenchymal stem cells. Here, the author showed that both vinexin α and CAP are required for the vinculin stabilization on rigid substrates and the promotion of the ECM stiffness-dependent YAP/TAZ nuclear localization. CAP functioned as a mechanosensor to regulate stiffness dependency of MSC differentiation, although vinexin predominantly promoted the differentiation into adipocyte in any stiffness of substrates. Collectively, these observations indicate that vinculin-SORBS family protein interaction plays important roles regulating ECM stiffness-dependent differentiation.

Here, the author demonstrated that vinexin and CAP regulated YAP/TAZ nuclear localization in an ECM stiffness-dependent manner. The author has revealed that vinculin regulates YAP/TAZ nuclear localization and P2 mutation of vinculin, which reduces interaction between vinculin and SORBS family proteins, attenuates this function in Chapter 1. In addition, the author's group recently revealed that vinexin and CAP share their function on ECM stiffness-dependent conformational changes of vinculin (1). Furthermore, Elosegui-Artola et al. reported

that talin unfolds and binds to vinculin on gels with above 5 kPa stiffness, resulting in the promotion of YAP nuclear translocation (16). These observations highlighted that vinculin-based focal adhesion complex plays essential roles in regulating ECM stiffness-dependent YAP/TAZ nuclear localization in mesenchymal cells.

It is intriguing that depletion of vinexin or CAP failed to induce a complete loss of ECM stiffness-dependent nuclear localization of YAP/TAZ in the range from 1.5 kPa to 8.7 kPa, rather depleted cells still promoted nuclear localization of YAP/TAZ moderately on 8.7 kPa. Two possible explanations for this moderate ECM stiffness-dependency of YAP/TAZ nuclear localization in vinexin- or CAP- depleted cells are as follows: First possibility is that there are other mechanosensors specific for soft range of stiffness. Talin experiences various intramolecular tension (17, 18). However, this tension is constant over the stiffness above 12 kPa (18), suggesting the presence of mechanosensors that dominantly function in the soft range of stiffness. Second possibility is that residual expression of vinexin and CAP in shRNA-mediated knockdown cells are sufficient to promote the nuclear localization of YAP/TAZ on moderately rigid substrates but not enough on rigid substrates. CRISPR/Cas9 system-mediated knockout of vinexin and CAP will be useful to circumvent this problem.

In the present study, the author showed that depletion of either vinexin or CAP abrogated the conformational changes of vinculin and nuclear localization of YAP/TAZ on rigid substrates, suggesting that ‘both’ vinexin and CAP are required for these regulations. It is possible that vinexin and CAP work cooperatively. Indeed, one of SORBS family protein, ArgBP2 is capable to bind another ArgBP2 molecule through association between its SH3 domain and a proline-rich cluster, leading to form oligomers to stimulate the association with binding partners (19). In addition, ArgBP2 and CAP could form a heterodimer. Furthermore, CAP variants form heterodimer among variants through their proline-rich region and coiled-coil domains (11). The

author's group also observed vinexin and CAP bind to tensin cooperatively (personal communication). Another possibility is that both vinexin and CAP bind to vinculin independently through different regions of vinculin to regulate vinculin status. Indeed, the author's group has recently identified a novel vinculin-head binding site in N-terminal region of vinexin α (personal communication).

In contrast to ST2 cells, in which both vinexin and CAP are required, the previous study showed that vinculin requires 'either' vinexin or CAP for its ECM stiffness-dependent conformational change in triple SORBS proteins KO/KD MEFs re-expressing one of SORBS protein (1). This discrepancy might be ascribed to the different cell context between MEFs and MSCs. Another possible reason is over-expression of SORBS proteins in Triple KO/KD cells compared to physiological expression. The re-expression of SORBS proteins in Triple KO/KD MEFs were higher than that in wild-type MEFs (1). The abundant expression might be sufficient to function with single SORBS proteins. On the other hand, here the author tested the effect of vinexin and CAP by depleting each protein and rescuing the effect by re-expression. Future study should investigate these possibilities.

It is still unclear how vinexin α and CAP regulate nuclear localization of YAP/TAZ. Hippo pathway is a well-known regulator of YAP/TAZ (20). The author checked the phosphorylation of YAP and LATS, a kinase phosphorylating YAP/TAZ in Hippo pathway. However, the author did not observe the significant changes in either phosphorylations (data not shown). In addition, the linkage between focal adhesion, actin-cytoskeleton and nuclear skeleton plays essential roles to regulate nuclear translocation of YAP/TAZ (15, 16, 21-23). The author has shown that actin-binding ability of vinculin is required for YAP/TAZ nuclear localization in Chapter 1. Depletion of vinexin and CAP also slightly increased the G-actin ratio (data not shown), suggesting the possibility that vinexin and CAP regulate YAP/TAZ nuclear localization through

the actin cytoskeleton. Previous reports have shown that vinexin and CAP contribute to the aggregation of stress fiber at focal adhesions (12, 24) support this idea. Furthermore, CAP affects Rho-family small GTPases, Cdc42 and TC10 activity (25). Cdc42 promotes YAP nuclear localization in mouse embryonic fibroblasts, embryonic kidney, and lung epithelia (26, 27). Thus, it will be an intriguing question whether vinexin or CAP regulates Rho-family small GTPases in MSCs to promote YAP/TAZ nuclear localization through actin dynamics. Lastly, it is possible that vinexin and CAP regulate YAP/TAZ nuclear localization through kinases, such as ERK. Vinexin and CAP directly bind to ERK (28, 29). In addition, Hwang and others reported ERK regulates nuclear localization of YAP/TAZ downstream of ECM stiffness in hMSCs (30). Further investigation is required to address how vinexin and CAP regulate the nuclear localization of YAP/TAZ.

Another important finding in this study is that CAP as well as vinculin suppresses adipocyte differentiation and promotes osteoblast differentiation. Using refined high content image analysis, Holle et al. have revealed that CAP is a novel candidate for a regulator of osteogenic differentiation (28). The author's finding that CAP promoted the osteoblast differentiation in a phenotypic level, and increased ALP activity and calcification, are consistent to this report. It is reported that CAP regulates insulin-dependent glucose uptake via c-Cbl interaction to promote GLUT4 trafficking in 3T3-L1 adipocyte cells (6, 7). This study extended our understanding of CAP function in the regulation of cell differentiation and revealed that CAP directs the lineage commitment of MSCs.

To the best of the author's knowledge, this study is the first report to demonstrate that vinexin promotes adipocyte differentiation and inhibits osteoblast differentiation. Considering the role of vinexin as ECM-stiffness sensor, which contributes to the cytoskeletal association of vinculin and promotion of YAP/TAZ nuclear localization, it was surprising that vinexin promotes

adipocyte differentiation on rigid (plastic) substrates. Many reports show the interaction of vinexin with various signaling molecules, including Sos, ERK, and non-receptor tyrosine kinase c-Abl (29, 31, 32). One candidate that mediates the adipocyte differentiation would be c-Abl, because activation of c-Abl promotes adipocyte differentiation by direct binding to PPARγ in 3T3-L1 adipocytes (33). Further investigation should be needed for the vinexin-dependent promotion of adipogenesis in MSCs.

In summary, the author concluded that vinexin and CAP, vinculin-linker binding partners, are involved in mechanosensing and promotes the ECM stiffness-dependent nuclear localization of YAP/TAZ. Together with Chapter 1, vinculin-CAP complex works as a mechanosensor to regulate ECM stiffness-dependent differentiation of MSCs into adipocytes via promoting nuclear localization of YAP/TAZ. In contrast, vinexin regulates the differentiation, independently of YAP/TAZ pathway.

MATERIALS AND METHODS

Plasmid construction

The small hairpin RNA for vinexin (#1 5'-GGTGAACGAACATTGGTATGA-3', or #2 5'-CGGCTCAGGCTTTGTGATGATGG-3') or CAP (#1 5'-GGACCTCCTCAATATAGAT GA-3', or #2 5'-GGAGACGTTGTTTACATCTAC-3') were subcloned into pLKO.1-Puro vector from Open Biosystems (Huntsville, AL). Expression plasmids containing mouse vinexin and CAP cDNA were described previously (1, 2). The cDNAs encoding vinexin and CAP resistant to shRNAs were generated by site-directed mutagenesis using In-Fusion® HD cloning kit (Clontech, Mountain View, CA) and subcloned into pCDH-EF1-IRES-hygro vector from System Biosciences (Mountain View, CA).

Antibodies and Reagents

Mouse anti-vinculin (V9131, dilution ratio: 1/20,000 (WB), 1/500 (IF)), rabbit anti-CAP (SORBS1) (HPA027559, 1/2,000 (WB), 1/100 (IF)) and anti-β−tubulin (T4026, 1/2,000) antibodies were purchased from Sigma (Saint Louis, MO). Mouse anti-β-actin antibody (ab6276, 1/10,000) was purchased from Abcam (Cambridge, UK). Mouse anti-YAP (sc-101199, 1/100 (IF), 1/1000 (WB)), and rabbit anti-ERK2 (sc-154, 1/10,000) were purchased from Santa Cruz Biotechnology (Santa Cruz, CA). Rabbit anti-aP2 (#3544, 1/2,000), anti-phospho ERK1/2 (1/1,000), anti-phospho YAP (#4911, 1/1,000), anti-LATS1 (#3477, 1/1,000), and anti-phospho LATS1 (#9157, 1/1,000) antibodies were purchased Cell Signaling Technology (Boston, MA). Mouse anti-FAK (1/1,000) and anti-phospho FAK (1/1,000) antibodies were purchased from BD Transduction laboratories (San Jose, CA). Rabbit anti-vinexin and anti-ArgBP2 polyclonal antibodies were described previously (1, 12). Alexa Fluor 568 phalloidin and 633 phalloidin was purchased from Thermo Fisher Scientific (Rockford, IL). Type I collagen was purchased from Nitta Gelatin (Osaka, Japan). Insulin and 3-Isobutyl-1-methylxanthine (IBMX) were purchased from Sigma. U0126 were purchased from Cell Signaling Technology.

Cell culture and differentiation

ST2, a mouse bone-marrow derived mesenchymal stem cell line, was obtained from RIKEN BRC (Tsukuba, Japan). ST2 cells were maintained in RPMI1640 (Sigma) supplemented with 10% fetal bovine serum (FBS; Sigma) at 37°C under a humidified atmosphere containing 5% CO_2. Polyacrylamide gel substrates are prepared as described in Chapter 1. The elastic moduli of the gels were from 1.5 kPa to 42 kPa. Adipocyte differentiation was performed as described in Chapter 1. Osteoblast differentiation was induced by cultured with αMEM (Sigma) containing 50 μg/ml ascorbic acid, followed by changing medium every 2 days.

Establishment of vinexin- or CAP- depleted cells and re-expressing cells

Vinexin- or CAP-depleted cells and vinexin α or CAP re-expressing cells were established using lentivirus as described previously (2). Briefly, lentiviruses were generated by transfecting pMD2.G, psPAX2, pRSV-Rev, pMDLg/pRRE (Addgene, Cambridge, MA), and pLKO.1 vectors (for knockdown) or pCDH vectors (for expression) to HEK293T cells using Lipofectamine® LTX and PLUS™ Reagent (Thermo Fisher Scientific). Cells were infected with lentiviruses, followed by incubating with the medium containing 1 μg/ml puromycin or 100 μg/ml hygromycin B.

siRNA-mediated knockdown

ST2 cells were transfected with 2 nM Stealth™ RNAi siRNAs against TAZ (siTAZ#1 5'-GGAAGGUGAUGAAUCAGCCUCUUGG-3', siTAZ#2; 5'-GGAGUCCUUCUUUAAGGAGCCCGAU-3'; Invitrogen, Carlsbad, CA), YAP (5'-CCAAGACAUCUUCUGGUCAAAGAUA-3'; Invitrogen) or control siRNA (Stealth™ RNAi Negative Control Medium GC Duplex#3, Cat. No. 12935-113) using Lipofectamine® RNAiMAX Reagent (Invitrogen). Lipofectamine complex were diluted 500 μl of OPTI-MEM (Gibco) and reverse transfected into 1.0×10^5 cells in 6 well plate. The medium was changed 24 hours after transfection.

Oil Red O, ALP activity, and Alizarin Red S staining and quantification

Oil Red O staining was performed as described in Chapter 1. ALP staining was performed with TRACP & ALP double-stain kit (TaKaRa, Ohtsu, Japan). For Alizarin Red S staining, cells were fixed with 10% formalin solution for 15 min. After washing with distilled water, cells were stained with 1% Alizarin Red S solution (Sigma) (pH 6.37 in ammonia solution)

for 30 min. After washing with distilled water, stained images were obtained by microscopy (Nikon ECLIPSE TE300-2) equipped with Leica MC120. For Oil Red O staining and Alizarin red S staining, stained area per total area were quantified by ImageJ. For ALP staining, stained intensity per image were quantified.

Quantitative real-time PCR (qRT-PCR)

qRT-PCR was performed as described in Chapter 1 with slight modification. Briefly, total RNA was extracted using RNeasy mini Kit (QIAGEN, Hilden, Germany), and cDNA was synthesized using Super Script reverse transcriptase III (Invitrogen). qRT-PCR analysis was carried out with Step One™ Real-Time PCR Systems (Applied Biosystems) using THUNDERBIRD® SYBR qPCR Mix (TOYOBO, Osaka, Japan). Relative expression levels to internal control 36B4 were given.

Immunostaining and quantification of FAs and YAP/TAZ nuclear localization

Immunostaining and quantification were performed as described in Chapter 1. Briefly, to analyze total vinculin, cells were fixed with 1.5% paraformaldehyde at RT for 45 min, followed by permeabilization with PBS containing 0.2% Triton X-100 for 5 min at room temperature. To analyze CSK-resistant vinculin, cells were first treated twice with CSK buffer (0.1% Triton X-100, 10 mM PIPES, pH 6.8, 50 mM NaCl, 3 mM $MgCl_2$, 300 mM sucrose) at 4°C for 30 sec, followed by 4% paraformaldehyde fixation with paraformaldehyde at room temperature. Images were obtained with LSM700 confocal microscope (Carl Zeiss, Oberkochen, Germany) with a ×40 Plan-APOCHROM objective lens. To obtain quantified data from single cells, neighboring cells in the images were erased. To analyze YAP/TAZ nuclear localization, cells were fixed with 4% paraformaldehyde and permeabilized with PBS containing 0.2% Triton X-100 for 5 min at room

temperature. Images were obtained with LSM700 confocal microscope with a ×40 Plan-APOCHROM objective lens, or with a Nikon C2 confocal microscope (Nikon, Tokyo, Japan) with a ×40 Plan-APO objective lens. Intensity of the same area in nucleus and cytosol were quantified and nucleus-to-cytosol intensity ratio was calculated.

Statistical analysis

Statistical analysis was performed using Origin 2017 software. Values according to the normal distribution were analyzed with Tukey's honest significant difference test, one-way ANOVA and Student's t-test for comparison among three or more groups and between two, respectively. Values not according to the normal distribution were analyzed with Mann-Whitney U-test after Kruskal Wallis's ANOVA for comparison among three or more groups.

REFERENCES

1. Ichikawa T, *et al.* (2017) Vinexin family (SORBS) proteins play different roles in stiffness-sensing and contractile force generation. *J Cell Sci* 130(20):3517-3531.
2. Yamashita H, *et al.* (2014) The role of the interaction of the vinculin proline-rich linker region with vinexin α in sensing the stiffness of the extracellular matrix. *J Cell Sci* 127(Pt 9):1875-1886.
3. Kioka N, Ueda K, & Amachi T (2002) Vinexin, CAP/ponsin, ArgBP2: a novel adaptor protein family regulating cytoskeletal organization and signal transduction. *Cell Struct Funct* 27(1):1-7.
4. Chen K, *et al.* (2013) Vinexin-β protects against cardiac hypertrophy by blocking the Akt-dependent signalling pathway. *Basic Res Cardiol* 108(2):338.
5. Kioka N, *et al.* (2010) Crucial role of vinexin for keratinocyte migration in vitro and epidermal wound healing in vivo. *Exp Cell Res* 316(10):1728-1738.
6. Ribon V, Printen JA, Hoffman NG, Kay BK, & Saltiel AR (1998) A novel, multifuntional c-Cbl binding protein in insulin receptor signaling in 3T3-L1 adipocytes. *Mol Cell Biol* 18(2):872-879.
7. Baumann CA, *et al.* (2000) CAP defines a second signalling pathway required for insulin-stimulated glucose transport. *Nature* 407(6801):202-207.
8. Lesniewski LA, *et al.* (2007) Bone marrow-specific Cap gene deletion protects against

high-fat diet-induced insulin resistance. *Nat Med* 13(4):455-462.

9. Anekal PV, Yong J, & Manser E (2015) Arg kinase-binding protein 2 (ArgBP2) interaction with α-actinin and actin stress fibers inhibits cell migration. *J Biol Chem* 290(4):2112-2125.
10. Zhang Q, *et al.* (2016) Impaired Dendritic Development and Memory in Sorbs2 Knock-Out Mice. *J Neurosci* 36(7):2247-2260.
11. Zhang M, Kimura A, & Saltiel AR (2003) Cloning and characterization of Cbl-associated protein splicing isoforms. *Mol Med* 9(1-2):18-25.
12. Kioka N, *et al.* (1999) Vinexin: a novel vinculin-binding protein with multiple SH3 domains enhances actin cytoskeletal organization. *J Cell Biol* 144(1):59-69.
13. Kuroda M, Wada H, Kimura Y, Ueda K, & Kioka N (2017) Vinculin promotes nuclear localization of TAZ to inhibit ECM stiffness-dependent differentiation into adipocytes. *J Cell Sci* 130(5):989-1002.
14. Engler AJ, Sen S, Sweeney HL, & Discher DE (2006) Matrix elasticity directs stem cell lineage specification. *Cell* 126(4):677-689.
15. Dupont S, *et al.* (2011) Role of YAP/TAZ in mechanotransduction. *Nature* 474(7350):179-183.
16. Elosegui-Artola A, *et al.* (2016) Mechanical regulation of a molecular clutch defines force transmission and transduction in response to matrix rigidity. *Nat Cell Biol* 18(5):540-548.
17. Ringer P, *et al.* (2017) Multiplexing molecular tension sensors reveals piconewton force gradient across talin-1. *Nature Methods* 14(11):1090-+.
18. Austen K, *et al.* (2015) Extracellular rigidity sensing by talin isoform-specific mechanical linkages. *Nat Cell Biol* 17(12):1597-1606.
19. Roignot J, Bonacci T, Ghigo E, Iovanna JL, & Soubeyran P (2014) Oligomerization and Phosphorylation Dependent Regulation of ArgBP2 Adaptive Capabilities and Associated Functions. *Plos One* 9(1):13.
20. Zhao B, *et al.* (2007) Inactivation of YAP oncoprotein by the Hippo pathway is involved in cell contact inhibition and tissue growth control. *Genes Dev* 21(21):2747-2761.
21. Wada K, Itoga K, Okano T, Yonemura S, & Sasaki H (2011) Hippo pathway regulation by cell morphology and stress fibers. *Development* 138(18):3907-3914.
22. Aragona M, *et al.* (2013) A mechanical checkpoint controls multicellular growth through YAP/TAZ regulation by actin-processing factors. *Cell* 154(5):1047-1059.
23. Elosegui-Artola A, *et al.* (2017) Force Triggers YAP Nuclear Entry by Regulating Transport across Nuclear Pores. *Cell* 171(6):1397-1410.e1314.
24. Zhang M, *et al.* (2006) CAP interacts with cytoskeletal proteins and regulates adhesion-

mediated ERK activation and motility. *EMBO J* 25(22):5284-5293.

25. Chiang SH, *et al.* (2001) Insulin-stimulated GLUT4 translocation requires the CAP-dependent activation of TC10. *Nature* 410(6831):944-948.
26. Reginensi A, *et al.* (2013) Yap- and Cdc42-dependent nephrogenesis and morphogenesis during mouse kidney development. *PLoS Genet* 9(3):e1003380.
27. Liu Z, *et al.* (2016) MAPK-Mediated YAP Activation Controls Mechanical-Tension-Induced Pulmonary Alveolar Regeneration. *Cell Rep* 16(7):1810-1819.
28. Holle AW, *et al.* (2016) High content image analysis of focal adhesion-dependent mechanosensitive stem cell differentiation. *Integr Biol (Camb)* 8(10):1049-1058.
29. Mitsushima M, Suwa A, Amachi T, Ueda K, & Kioka N (2004) Extracellular signal-regulated kinase activated by epidermal growth factor and cell adhesion interacts with and phosphorylates vinexin. *J Biol Chem* 279(33):34570-34577.
30. Hwang JH, *et al.* (2015) Extracellular Matrix Stiffness Regulates Osteogenic Differentiation through MAPK Activation. *PLoS One* 10(8):e0135519.
31. Mitsushima M, Takahashi H, Shishido T, Ueda K, & Kioka N (2006) Abl kinase interacts with and phosphorylates vinexin. *FEBS Lett* 580(17):4288-4295.
32. Akamatsu M, *et al.* (1999) Vinexin forms a signaling complex with Sos and modulates epidermal growth factor-induced c-Jun N-terminal kinase/stress-activated protein kinase activities. *J Biol Chem* 274(50):35933-35937.
33. Keshet R, *et al.* (2014) c-Abl tyrosine kinase promotes adipocyte differentiation by targeting PPAR-gamma 2. *Proc Natl Acad Sci U S A* 111(46):16365-16370.

SUMMARY

Mesenchymal stem cells (MSCs) are multipotent stem cells with the capacity to differentiate into various types of cells, including adipocytes, myoblasts, chondrocytes, and osteoblast. In addition to soluble factors, such as TGF-β or retinoic acid, MSC lineages specifications can be directed by physical cues including the extracellular matrix (ECM)-stiffness. For example, MSCs cultured on soft substrates differentiate into adipocytes efficiently, whereas cells on rigid substrates preferentially differentiate into osteoblasts. However, the underlying molecular mechanisms have been largely unclear. Cell-ECM adhesion sites, called focal adhesions (FAs), play important roles in sensing ECM stiffness and transducing the information into downstream signaling molecules. On rigid ECM, cells generate higher contractile force through their actomyosin system and thus conformational changes of focal adhesion proteins occur to transduce signals. It has been previously revealed that vinculin, an F-actin binding focal adhesion protein, changes its conformation to F-actin high-affinity form on rigid ECM. Furthermore, this conformational change requires binding to vinexin α (SORBS3) and CAP (SORBS1). In the present study, the author revealed that mechanism of the ECM stiffness-dependent differentiation of MSCs focusing on vinculin and SORBS family proteins.

In Chapter 1, the author found that rigid ECM changes vinculin conformation to actin-high affinity form in MSCs. In addition, vinculin promoted nuclear localization of YAP/TAZ to inhibit adipocyte differentiation on rigid ECM, resulting in MSC differentiation to adipocytes in a manner dependent on ECM stiffness. Furthermore, this regulation involved actin-binding ability of vinculin.

In Chapter 2, the author found that both vinexin α and CAP were required for the conformational changes of vinculin to actin-high affinity form. Furthermore, both vinexin α and CAP promoted the ECM-stiffness dependent nuclear localization of YAP/TAZ and regulated the ECM stiffness-dependent differentiation. In addition, CAP, as well as vinculin, suppressed the differentiation into adipocytes on rigid ECM, whereas vinexin α promoted the differentiation into adipocytes, independently of YAP/TAZ localization and ECM stiffness.

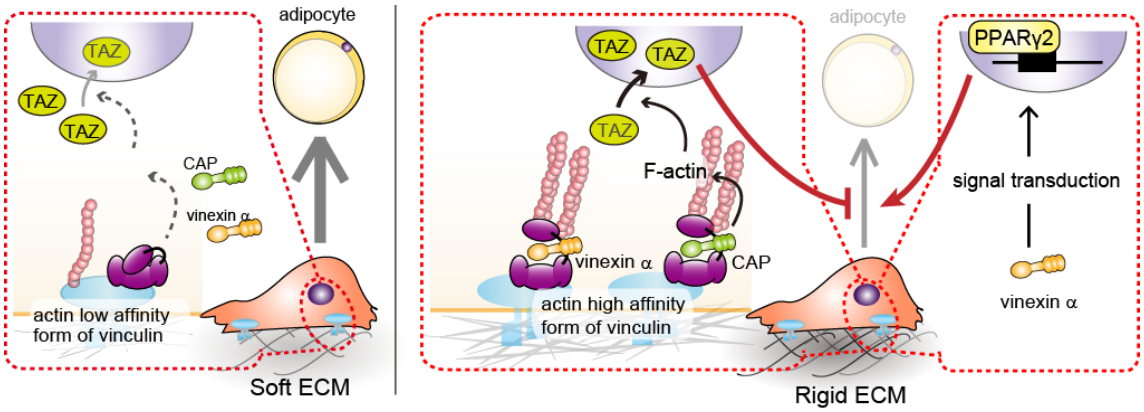

Fig. 1 Schematic models of ECM stiffness-dependent differentiation of mesenchymal stem cells

From these results, the author proposes a model to explain how rigid ECM suppress the differentiation into adipocytes (Fig. 1). On soft ECM, the vinculin head-tail interaction inhibits the association with F-actin and SORBS family proteins (vinexin and CAP) at FA. YAP/TAZ, especially TAZ, remain in the cytosol and MSCs differentiate into adipocytes, but not into osteoblasts. On rigid ECM, vinculin changes its conformation to actin-high affinity form, which requires the interaction of SORBS family proteins. Vinculin-SORBS family proteins promote TAZ nuclear translocation via the actin cytoskeleton and suppress adipocyte differentiation. In addition, vinexin α promotes MSC differentiation into adipocytes through signal pathways distinct from YAP/TAZ.

LIST OF PUBLICATIONS

1. Mito Kuroda, Hiroki Wada, Yasuhisa Kimura, Kazumitsu Ueda, and Noriyuki Kioka
"Vinculin Promotes Nuclear Localization of TAZ to Inhibit ECM Stiffness-Dependent Differentiation into Adipocytes."

Journal of Cell Science, 130, 989-1002, March 1, 2017
doi: 10.1242/jcs.194779

2. Mito Kuroda, Kazumitsu Ueda, and Noriyuki Kioka
"Vinexin family (SORBS) proteins, regulate the differentiation of mesenchymal stem cells."

In preparation

Related Publications

1. Takashi Fukada, Sakajiri H., Mito Kuroda, Noriyuki Kioka, Kenji Sugimoto
"Fluid shear stress applied by orbital shaking induces MG-63 osteosarcoma cells to activate ERK in two phases through distinct signaling pathways"

Biochemistry and Biophysics Reports, 9:257-265, 2017
doi: 10.1016/j.bbrep.2017.01.004

ACKNOWLEDGEMENTS

I would like to express sincere appreciation to Professor Dr. Kazumitsu Ueda, Laboratory of Cellular Biochemistry, Division of Applied Life Science, Graduate School of Agriculture, Kyoto University, who provided kind guidance and invaluable advice throughout this work.

I am deeply grateful to my supervisor, Associate Professor Dr. Noriyuki Kioka, Laboratory of Cellular Biochemistry, Division of Applied Life Science, Graduate School of Agriculture, Kyoto University, for his kind guidance and warm encouragement through the whole course of this work. The discussions with Dr. N. Kioka always gave insightful comments and inestimable suggestions to this work.

I appreciate for Dr. Ichiro Harada (Tokyo Institute of Techonology) for providing technical instructions of preparing polyacrylamide gels, and Ms. Yuki Wantani for providing valuable materials. I thank to Mr. Hiroki Wada for his great effort to the initial stage of my work.

I thank to members of Laboratory of Cellular Biochemistry for their constant support; notably, Dr. Yasuhisa Kimura provided this work with valuable comments and suggestions.

Finally, I would like to express deep gratitude to my family for their continuous support and encouragement.

March 2018

Mito KURODA